OXFORD

ORIGINAL ARTICLE

Anti-Myelin Proteolipid Protein Peptide Monoclonal Antibodies Recognize Cell Surface Proteins on Developing Neurons and Inhibit Their Differentiation

Raymond A. Sobel, MD, Mary Jane Eaton, MA, Prajakta Dilip Jaju, MD, Eugene Lowry, MD, and Julian R. Hinojoza, BS

Abstract

Using a panel of monoclonal antibodies (mAbs) to myelin proteolipid protein (PLP) peptides, we found that in addition to CNS myelin, mAbs to external face but not cytoplasmic face epitopes immunostained neurons in immature human CNS tissues and in adult hippocampal dentate gyrus and olfactory bulbs, that is neural stem cell niches (NSCN). To explore the pathobiological significance of these observations, we assessed the mAb effects on neurodifferentiation in vitro. The mAbs to PLP 50–69 (IgG$_{1\kappa}$ and IgG$_{2a\kappa}$), and 178–191 and 200–219 (both IgG$_{1\kappa}$) immunostained live cell surfaces and inhibited neurite outgrowth of E18 rat hippocampal precursor cells and of PC12 cells, which do not express PLP. Proteins immunoprecipitated from PC12 cell extracts and captured by mAb-coated magnetic beads were identified by GeLC-MS/MS. Each neurite outgrowth-inhibiting mAb captured a distinct set of neurodifferentiation molecules including sequence-similar M6 proteins and other unrelated membrane and extracellular matrix proteins, for example integrins, Eph receptors, NCAM-1, and protocadherins. These molecules are expressed in adult human NSCN and are implicated in the pathogenesis of many chronic CNS disease processes. Thus, diverse anti-PLP epitope autoantibodies may inhibit neuronal precursor cell differentiation via multispecific recognition of cell surface molecules thereby potentially impeding endogenous neuroregeneration in NSCN and in vivo differentiation of exogenous neural stem cells.

Key Words: Antibody multispecificity, Autoimmunity, Immunoprecipitation, Multiple sclerosis, Myelin proteolipid protein, Neural stem cell, Neurodegeneration.

INTRODUCTION

Myelin proteolipid protein (PLP) is the most abundant myelin protein in the mammalian CNS (1, 2). It is a polytopic, integral membrane protein with extracellular and cytoplasmic domains. PLP is a member of the proteolipid gene family (pgf), of which the minor component of mammalian CNS myelin DM-20 is the ancestral gene transcript. To dissect polyclonal anti-PLP antibody (Ab) responses that may occur in pathological conditions in vivo, we generated and characterized a panel of monoclonal antibodies (mAbs) that recognize epitopes in regions of PLP located on the cytoplasmic and external membrane faces of the molecule (3). In addition to the expected immunostaining of nonhuman vertebrate CNS tissue myelin, several of the mAbs also immunostained multiple neuron populations in many CNS regions. Although the neuronal epitopes recognized and their conformations in vivo are not known, the mAb recognition of both myelin and neurons appeared to correlate with the extent of conservation of known pgf member sequences in the various species tested. This suggested that anti-PLP Abs might similarly recognize evolutionarily conserved epitopes expressed in neurons as well as in CNS myelin in the human CNS and that this might have pathobiological significance in human diseases.

To investigate these questions, we analyzed the capacity of the mAbs to recognize myelin and other cells in samples from normal human CNS tissues from subjects of different developmental stages using immunohistochemistry (IHC). The patterns of neuronal recognition differed from those of developing CNS myelin in that neuronal recognition by the mAbs was more frequent in samples from normal prenatal and early postnatal subject tissue samples than in adult CNS neurons. The mAbs also immunostained immature-appearing and cells with neuronal morphology in adult neural stem cell niches (NSCN), that is hippocampal dentate gyrus and olfactory bulb (4, 5). This suggested that the anti-PLP Abs may recognize functionally relevant neurodevelopmental molecules throughout life in humans and that the neuronal epitope recognition differs from that of myelin recognition in vivo.

Glycoproteins M6a and M6b are pgf proteins with sequence similarities with PLP; they also likely evolved from the primordial DM-20 (6–8). M6 proteins are expressed in both myelinating and non-myelinating cells, including

neurons, and are critical for vertebrate CNS development (9–15). Because an anti-M6 mAb had been shown to inhibit in vitro neurite outgrowth (9), we hypothesized that the anti-PLP mAbs would also recognize sequence-similar pgf proteins such as M6 proteins expressed on developing neuronal cells and have effects comparable to those of the anti-M6 mAb. We identified anti-PLP mAbs that inhibited in vitro neurite outgrowth in 2 in vitro models of neuron differentiation and then identified multiple cell surface and extracellular matrix (ECM) molecules with and without sequence similarity with PLP that are expressed by differentiating neuronal cells and were captured by the neurite outgrowth-inhibiting mAbs in immunoprecipitation (IP) experiments. We then confirmed the expression of some of these mAb targets in adult human NSCN.

To our knowledge, these findings represent the first report of immune recognition of multiple cell surface neuronal developmental antigens by any anti-myelin epitope mAb. Because anti-PLP antibodies may be generated following CNS myelin breakdown in demyelinating diseases (primary demyelination), as in multiple sclerosis (MS), following infarction and traumatic lesions, and in chronic aging-related neurodegenerative processes, (i.e. secondary demyelination), our findings lead to the hypothesis that certain anti-PLP autoantibodies can inhibit the growth and differentiation of neuronal precursor cells through multispecific ("promiscuous") binding thereby impairing CNS neuron regeneration in vivo. This suggests a novel mechanism for impaired functional recovery in many chronic pathological processes affecting the postnatal and adult human CNS.

MATERIALS AND METHODS

Antibodies

The anti-PLP and anti-M6 protein Abs and the dilutions used are listed in Table 1. The epitopes of the mAbs and their locations are depicted in a model of the PLP molecule (Fig. 1). The sequences of the epitopes recognized by the mAbs are presented in Supplementary Data Table S1. Additional antibodies used for characterization of expression of identified anti-PLP mAb targets fixed rat hippocampal precursor cells (RHPC) and PC12 cells and in adult NSCN are listed in Table 2.

Human CNS Tissue Samples

Human formalin-fixed paraffin-embedded (FFPE) CNS tissue samples from subjects from early developmental stages to adults who died of non-neurological conditions were immunostained with the anti-PLP mAbs and other Abs (Supplementary Data Table S2A, B). Paraffin block samples were obtained from the archives of the Stanford University School of Medicine Department of Pathology (Stanford, CA). Additional sample blocks were obtained from archives of the Laboratory Service of the Palo Alto Veterans Affairs Health Care System (Palo Alto, CA) and the Human Brain and Spinal Fluid Resource Center (Los Angeles, CA). For analyses of NSCN, samples of hippocampi and olfactory bulbs from normal adults (of various ages), and from adults with Alzheimer disease and hypoxic-ischemic neuronal injury were used (Supplementary Data Table S2C). FFPE blocks from 2 patients with chronic MS were also used for determination of mAb recognition of axons in acute and chronic white matter lesions (Supplementary Data Table S2D). Information on age at death, gender, neuropathologic diagnosis, major cause of death, and postmortem intervals were obtained from autopsy reports. The samples were analyzed using study code numbers; no personal identifiers were retained or used in the analyses. The experimental protocols for analyses of archival paraffin tissues were exempt from formal Human Studies Committee review at the time of collection.

TABLE 1. Anti-PLP and Anti-M6b Antibodies*

Antibody Name	PLP Epitope	Isotype	Dilution Used for Immunostaining of FFPE Tissues (With Antigen Retrieval)/Fixed Cells	Starting Concentration (μg/mL) for Live Cell Immunostaining of RHPC and PC12 Cells	Concentration for In Vitro Treatment (μg/mL) of RHPC/PC12 Cells
F4.4C2	50–69	Mouse IgG$_{1\kappa}$	(1:10)/(1:100)	1300	10/5
F3.9E9	50–69	Mouse IgG$_{2a\kappa}$	(1:50)/(1:100)	1000	10/5
2D2	100–123	Mouse IgG$_{1\kappa}$	(1:100)/(1:100)	363	10/5
1C5	139–151	Mouse IgG$_{1\kappa}$	(1:50)/(1:50)	410	10[†]/ND
P7.6A5	178–191	Mouse IgG$_{1\kappa}$	(1:50–1:200)/(1:100)	699	10/5
F4.8A5	200–219	Mouse IgG$_{1\kappa}$	(1:100)/ND	300	10/5
P5.12A8	264–276	Mouse IgM	(1:50)/ND	170	10[†]/ND
AA3	264–273	Rat IgG$_{2b}$	(1:100)/ND	Not determined	ND/ND
M6[‡]	NA	Rat IgG$_{2a}$	ND/1:10	26	10/5
GPM6b[§]	NA	Rabbit polyclonal	1:100–1:200/1:100	Not determined	ND/ND

*Generation and characterization of anti-PLP mAbs are described in Greenfield et al (3) and Yamamura et al (16) and were kindly provided by Vijay K. Kuchroo and Nassim Kassam (Harvard Medical School, Boston, MA).
[†]Treatment of RHPC only.
[‡]Supernatant from Developmental Studies Hybridoma Bank, University of Iowa, Iowa City, IA used for immunostaining and in vitro treatment of RHPC and PC12 cells.
[§]Antibody ab214459 from Abcam (Cambridge, MA) used for immunostaining of PC12 cells and FFPE tissues.
FFPE, formalin-fixed, paraffin-embedded; MBP, myelin basic protein; NA, not applicable; ND, not done; RHPC, E18 rat hippocampal precursor cells.
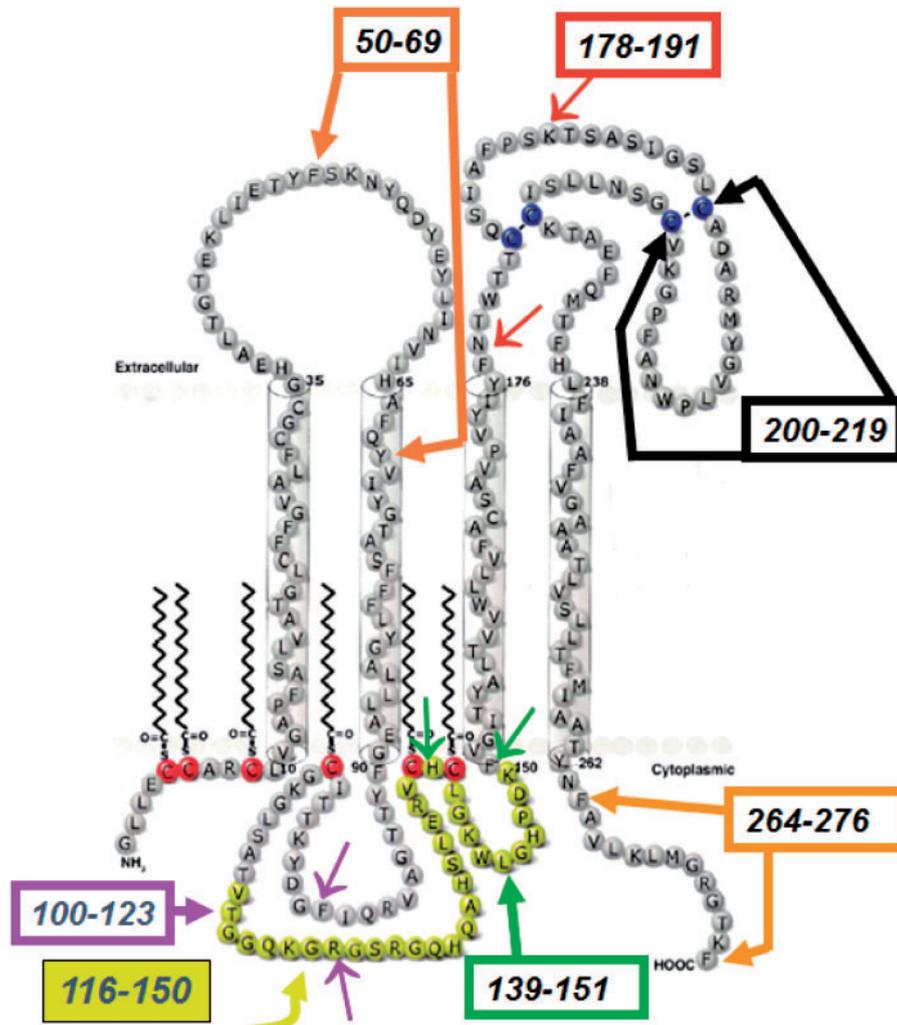
FIGURE 1. Schematic diagram of myelin proteolipid protein (PLP). Colored arrows delineate the peptide sequences to which the anti-PLP monoclonal antibodies used in this study are specific (3). The region indicated in yellow (residues PLP 116–150) is present in PLP but is not present in DM-20 or other proteolipid gene family proteins; it is, therefore, PLP-specific. The diagram is based on Figure 1 in (1) and is used with permission from Elsevier.

Immunohistochemistry

Six- to 8-µm-thick sections of CNS tissues from paraffin blocks were cut and placed on Superfrost plus microscope slides (Thermo Fisher Scientific, Waltham, MA); the slides were then deparaffinized in xylenes, rehydrated in graded alcohols to 95% ethanol and washed 3 times in phosphate-buffered saline (PBS), pH 7.4. Antigen retrieval was performed by microwaving the slides in 10 mM citrate buffer, pH 6.0, 4 minutes at 1000 W and 11 minutes at 800 W, topping off after 7, 4, and 1 minute, and cooling at room temperature (RT) uncovered for 30 minutes. The slides were then rinsed twice in deionized water. Endogenous peroxidase activity was quenched by exposure to 0.3% H_2O_2 in PBS for 10 minutes. After 3 10-minute washes in PBS, blocking with 1% normal goat, horse, or rabbit serum (Vector, Burlingame, CA), in PBS (for goat anti-rabbit Ig, horse anti-mouse IgG or IgM, or rabbit anti-rat Ig) secondary antibody, respectively) (175 µL/slide) for 10 minutes was performed in a humidified chamber at RT.

The slides were then incubated with primary antibody (50–100 µL/slide) (Tables 1 and 2), diluted in PBS overnight in the humidified chamber at 4°C. The following day, the slides were washed 3 times for 10 minutes in PBS and then incubated with the appropriate biotinylated secondary antibody (Vector) for 30 minutes in a humidified chamber at RT. After 3 10-minute washes in PBS, they were incubated with Vectastain Elite ABC reagent (Vector) for 45 minutes in humidified chamber at RT. Reaction product was visualized with 3,3′-diaminobenzidine (0.025 mg/50 mL PBS, filtered and 0.5 mL 3% H_2O_2 added). Duration of exposure for optimal visualization of reaction product was determined by direct observation of the slides under a microscope for each Ab. The slides were then washed 2 times for 5 minutes in PBS, post-fixed in 10% neutral buffered formalin for 10 minutes, and washed in deionized H_2O and then tap water for 1 minute each. They were then counterstained with hematoxylin (Sigma-Aldrich, St. Louis, MO) for 6 minutes, washed in H_2O, dehydrated in graded alcohols to

821

TABLE 2. Commercial Antibodies Used to Characterize Human Formalin-Fixed Paraffin-Embedded CNS Samples, E18 Rat Hippocampal Precursor Cells and PC12 Cells by Immunohistochemistry

Antigen	Clone Name	Isotype	Concentration Used for Immunostaining of Tissues/Cells	Source
EphA3	SAB2701156	Rabbit polyclonal	1:100/1:100	Sigma-Aldrich, St. Louis, MO
EphA10	HPA027497	Rabbit polyclonal	1:100/1:100	Sigma-Aldrich
EphB1	LS-C407798	Rabbit polyclonal	1:100/1:100	LifeSpan Biosciences, Inc., Seattle, WA
MBP	–	Rabbit polyclonal	Not determined*/ND	Cell Marque, Rocklin, CA
MBP 119-131	MAB381	Mouse IgG$_{2a}$	1:100/ND	Chemicon International, Temecula, CA
MBP 129-138	MAB382	Mouse IgG$_1$	1:100/ND	Chemicon International
Neurofilament heavy chain	NF200	Rabbit polyclonal	ND/1:100	Sigma-Aldrich
NCAM	AB5032	Rabbit polyclonal	1:500/1:100	Millipore, Billerica, MA
NrCAM	HPA012606	Rabbit polyclonal	1:50/1:100	Sigma-Aldrich
Protocadherin β12 (PCDHB12)	NPB1-77002	–	1:100/1:500	Novus Biologicals, Littleton, CO
Normal rabbit serum (control)	–		1:10–1:100/1:50–1:100	Vector Laboratories, Burlingame, CA

*Antibody purchased pre-diluted from supplier.
MBP, myelin basic protein; ND, not done.

xylenes and coverslipped with Permount (Thermo Fisher Scientific).

Analysis of Neuron Immunostaining in Human CNS Samples

All FFPE samples were stained with the Luxol fast blue-H&E or H&E stain and by immunohistochemistry with the anti-PLP mAb panel and 1 or both anti-myelin basic protein (MBP) mAbs. Because of rapid prenatal and early postnatal growth of the brain, the sizes of specific regions at different ages in early development were variable; there were also differences in regional tissue sampling at autopsy and in availability of specific anatomic regions, particularly of cerebral cortical regions. Initial analyses demonstrated that in the early developmental subject tissue samples there was greater immunostaining of neurons with the anti-PLP mAbs in the brainstem, cerebellum, and spinal cord versus more rostral regions. The caudal CNS regions could, therefore, be scored for immunopositivity of discrete neuron populations with greater precision. The extents of neuronal cytoplasmic or surface immunostaining were assessed in the following 17 regions (when available): cerebral cortex (n = 1), deep gray nuclei (i.e. basal ganglia or thalamus, n = 1), midbrain (n = 1), pons, (tegmentum and basis pontis, n = 2), medulla (dorsal cranial nerve X nucleus, cranial nerve XII nucleus, inferior olivary nucleus, arcuate nucleus, n = 4), cerebellum (internal granular layer, Purkinje cells, cerebellar molecular layer, external granular layer (when present), dentate nucleus, n = 5), and spinal cord, (anterior horn cells, other spinal neuron somata, dorsal root ganglia, and spinal nerve root myelin, n = 4). In each region for each subject and each mAb, neuronal staining was scored as follows: + (many neuron somata stained); ± (rare neurons or overall faint neuron staining in a single sample or in each of multiple adult samples; M (presence or absence of a diffuse staining blush in the cerebellar molecular layer (10); or 0 (no neurons stained or staining absent in cerebellar molecular layer).

E18 RHPCs

Primary E18 rat hippocampal cells (NeuroPure) were obtained from Gene Therapy Systems/Genlantis, San Diego, CA). Cells were dissociated using the neuropapain enzyme according to the Genlantis protocol and transferred to plating medium. They were plated onto poly-D-lysine-coated plastic 4 chamber slides at initial plating densities of 1×10^5 cells/mL. They were grown in Neurobasal/B27/0.5 mM glutamine/25 μM glutamate culture medium provided by the supplier and incubated at 37°C in 5% CO_2. On days 1, 3, or 7 of culture, the media was removed from each well and the cells were fixed with 10% neutral buffered formalin for immunohistochemistry.

Rat PC12 Cells

For PC12 cell cultures, sterile plastic Petri dishes (100 × 15 mm) and 4 chamber Permanox slide system wells (Fisher) were coated with type IV collagen (Sigma) dissolved in 0.25% sterile acetic acid at 1.45 μg/cm^2 overnight. The excess was then decanted, and the dishes and slides were stored covered aseptically at RT until they were used.

PC12 cells (CRL-1721.1, Lot 60131962) were obtained from the American Type Culture Collection (ATCC, Manassas, VA) in PC12 cell freezing medium (F); they were stored (1 mL/cryovial) in liquid nitrogen until use. PC12 cell medium components from ATCC were prepared with 500 mL F12K medium, 90 mL horse serum (15%), 15 mL fetal bovine serum (2.5%), with 6.1 mL (1%) penicillin-streptomycin solution (P0781, Sigma-Aldrich). The media was sterile filtered (0.2 μm filter) and stored at 2°–8°C until use. For experiments, the vials were thawed and the cells resuspended in 19 mL PC12 cell medium. They were then centrifuged (11 000 rpm) for 7 minutes at RT; the supernatant was decanted and discarded. The cell pellets were then resuspended in 10 mL PC12 cell medium, mixed, and transferred to collagen-coated plates or 4 chamber multiwell slides and incubated in humidity at 37°, 5% CO_2, either without or with 50 ng/mL nerve growth factor

(NGF). Media was aspirated and replaced every 48–72 hours until cells were near confluent as observed under an inverted microscope.

Routine Staining and Immunohistochemistry of RHPC and PC12 Cells

The same protocols as for paraffin sections were used for fixed preparations of RHPC and PC12 cells grown on multiwell plastic slides with several modifications: (i) There was no deparaffinization. (ii) After the cell cultures were fixed with the addition of 0.5 mL 10% neutral buffered formalin, they were stored at 2°–8° C until they were stained. (iii) For staining, the polystyrene media chambers were removed; the slides could then be stained routinely with hematoxylin or processed for immunohistochemistry. (iv) The antigen retrieval step was omitted. (v) After staining (or counterstaining) with hematoxylin, the water-based mounting medium Aqua Polymount (Polysciences, Inc., Warrington, PA), was applied prior to coverslipping. In all immunostaining experiments on cells, there was at least 1 control well in which PBS was substituted for Ab.

Immunolocalization ("Live Staining") Experiments of RHPC and PC12 Cells

To identify potential cell surface staining, sterile anti-PLP and -M6b mAbs (Table 1) were added to the culture wells and incubated for 2 hours. Control cultures were maintained in normal media. The culture wells were then washed in PBS, fixed in formalin and immunostained for bound Ab with horse anti-mouse IgG or IgM as secondary antibody. This permitted detection of Ig bound to the live cells before fixation. IHC was then performed, as described above for fixed preparations of cultured cells.

Antibody Effects on In Vitro Neurite Outgrowth of RHPC and PC12 Cells

Cells were suspended in growth media at $\sim 1 \times 10^5$ cells/mL and one of the anti-PLP or -M6 mAbs added (10 µg/mL for RHPC, 5 µg/mL for PC12 cells) and transferred to multiwell slides. They were incubated as described above for either 1 or 3 days (RHPC), or until control slides showed abundant neurite outgrowth (PC12 cells). They were then fixed and in formalin and counterstained with hematoxylin. In all treatment experiments, there was at least 1 control well in which normal media was used as a negative control.

Assessment of Neurite Outgrowth

Analyses of in vitro neurite outgrowth were performed on RHPC grown on slides from multiwell chamber cultures and on mAb-treated PC12 cells grown with NGF. From 7 to 10 fields (depending on cell density) of each experimental condition were photographed at ×40 magnification using a Nikon E1000M Eclipse microscope with an attached digital camera (Nikon, Melville, NY). Imaging software program (SPOT Imaging Solutions, Sterling Heights, MI), allowed calibration, (i.e. a 50 µm bar merged into the field), for neurite

length measurements. Fields that were selected for photographs had moderately high cell density, that is similar numbers of cells/field, but without extensive clustering or overlap that impeded neurite length measurements. JPG files were modified to optimize color balance, brightness, and contrast using Adobe Photoshop CS6 (Adobe Systems, Inc., San Jose, CA), without altering the appearance of the original materials. Each of the files was then printed on 8″ × 11″ paper and given a coded label. An observer blinded to the cell treatments first counted total numbers of nuclei in the fields. Because in NGF-treated control cultures, most cells had either nuclei or processes that touched other cells, the numbers of round cells not touching others and without cell processes, (i.e. undifferentiated cells), could be counted more easily than overlapping cells. The blinded observer then determined numbers of cells with neurite outgrowth (total cells-undifferentiated cells) and calculated percentages of cells with neurite outgrowth in each field (cells with neurite outgrowth/total). Elongated narrow processes, that is axons and dendrites, were identified in each photograph and their proximal and distal ends were then marked on the paper by a second blinded observer; lengths were then measured with a ruler by the first blinded observer and true lengths calculated based on the calibration bar in the field. In addition, the proportions of cells with neurite process lengths equal to or greater than 6.25 µm were also determined; results were essentially the same as those determined by the counting method described above.

Statistics

Proportions of cells with neurite outgrowth and process length data for each experiment (i.e. from each 4-well chamber) were analyzed using 1-way ANOVA with appropriate corrections; paired comparisons were analyzed with 2-tailed t test with appropriate corrections. Statistics were performed using GraphPad Prism 5 (GraphPad, Inc., La Jolla, CA).

Immunoprecipitation

PC12 cells were grown in collagen-coated Petri dishes with or without NGF, as described above. For harvesting, cell monolayers were rinsed briefly with ice cold 10 mM PBS, pH 7.2, and the washes discarded. Then, 0.5 mL PBS with 20 µL/mL protease inhibitor (PI, Halt PI, Thermo Fisher #78442) and 5 mM EDTA were added to each plate. The cells were then scraped and pooled into tubes. Cell suspensions were centrifuged at 5000g for 2 minutes at 4°C; an aliquot of the supernatant was saved for PAGE. The cell pellet was resuspended in 1 mL triple lysis buffer (50 mM TBS pH 7.4, 1% Triton X-100, 0.5% sodium deoxycholate, 0.1% sodium dodecyl sulfate, 1 mM EDTA, 5% glycerol) with 20 µL/mL PI and 1 mM EDTA, and incubated at 4°C with mixing by inversion for 30 minutes. This lysate was then centrifuged at 13 000g for 10 minutes at 4°C. An aliquot of cell debris was saved for PAGE. In some experiments, DDM lysis buffer (25 mM TBS, pH 7.4, 1% n-dodecyl maltoside glycerol, 5 mM EDTA in ultrapure H_2O) was used for cell lysis. All solutions were 0.2 µm filtered prior to use.

mAb crosslinking to magnetic beads, IP and elution procedures were performed using a Pierce Crosslink Magnetic IP/Co-IP Kit (Thermo Fisher No. 88805), according to the manufacturer's protocols. In all experiments, 5 μg/100 μL of mAb in coupling buffer were used for crosslinking to magnetic beads. Eluates (100 μL) from the beads were transferred to 0.5 mL microfuge tube with 11 μL neutralization buffer from the kit, mixed, and stored in liquid nitrogen.

Lithium Dodecyl Sulfate Polyacrylamide Gel Electrophoresis

Samples were prepared for analysis by lithium dodecyl sulfate (LDS) polyacrylamide gel electrophoresis (LDS-PAGE) using NuPAGE 4%–12% Bis-Tris Protein Gels (1.0 mm, 12 wells, Invitrogen) and recommended reagents (NuPAGE, Invitrogen). Samples (52 μL in 4× LDS buffer [20 μL] and 10× reducing agent [8 μL]) or the same buffer and reducing agent with ultrapure H_2O (52 μL) were heated at 100°C for 10 minutes. The upper chamber contained 200 mL running buffer (1× MES SDS running buffer [Thermo Fisher]), with anti-oxidant; the lower chamber contained 600 mL 1× MES. The gels were run in duplicate in an XCell Sure-Lock Mini-Cell system (Thermo Fisher) with Hoefer PS 500 XT DC power supply at 200 V constant. Separate lanes in the gels, included the initial crude sample supernatants, lysate, post-IP lysate, mAb control, protein molecular weight ladders (MagicMark XP Western Protein Standard, Thermo Fisher), mAb-coated beads, serial eluates from the beads, and post-eluate bead samples.

Transblot

One gel was transferred to 0.45 μm PVDF membranes (Pall Gelman Biotrace, Port Washington, NY) for Western-chemiluminescence using XCell II Blot Module (Thermo Fisher) with a Fisher Scientific FB300 power supply. The transblot buffer consisted of 25 mM TRIS, 102 mM glycine, 10% methanol with 500 μL antioxidant per 500 mL. Transblot was performed at 140 mA constants for 1.5 hours and 250 mA constant and for 30 minutes, both at 4°C.

Western Blot

PVDF membranes were washed 2 times for 5 minutes each with 25 mM TBS, pH 7.4, and placed into a stomacher bag. Blocking was performed by adding 20 mL blocking buffer (25 mM TBS, pH 7.4, 0.1% casein, 0.05% Tween 20) to the PVDF membranes and incubating 1 hour at RT with mixing. The excess was decanted and discarded. The membranes were incubated overnight with anti-PLP mAb (1:1000 dilution, 5 μg) in 5 mL blocking buffer at 2°–8°C and then 1 hour at RT. They were then washed 4 times for 5 minutes each with blocking buffer. The membranes were then incubated with goat anti-mouse horseradish peroxidase (HRP) (1:20 000, 0.5 μL in 10 mL blocking buffer), for 1 hour at RT with mixing. They were then washed 4 times for 5 minutes each in blocking buffer at RT with mixing, and 2 times briefly in TBS. The bound HRP was detected by incubating the membranes in the Working Solution (5 mL stable peroxide solution, 5 mL

Luminol/Enhancer solution from SuperSignal West Pico PLUS Chemiluminescent Substrate, Thermo Fisher) for 5 minutes at RT in the dark. Excess reagent was drained; membranes were placed in sheet protectors and exposed to CL-Xposure film (Thermo Fisher) from 2.5 to 7.5 minutes. Representative Western blots are shown in Supplementary Data Figures S1 and S2.

Silver Staining Analysis

The second gel was silver stained using mass spectrometry compatible kits (Pierce Silver Stain for Mass Spectrometry 24600 or Pierce #24612). Candidate bands that were identified in the Western blot were excised from the silver-stained gels for GeLC-MS/MS analysis. In some experiments, bands corresponding to Ab heavy and light Ig chains and uncoated (PBS) and post-elution bead samples, and bands in the gels from cell suspension, cell pellet, lysate, and post-IP lysate samples were also excised and analyzed for comparisons to samples from eluate bands as either negative or positive controls. Eluates from lysates of NGF-treated and -untreated samples were also compared in some experiments; in very few instances, however, proteins identified from NGF-untreated cell lysates were not identified in samples from NGF-treated lysates. In comparisons of the 2 anti-50–69 mAbs F4.4C2 and F3.9E9, bands at the same MW where 1 sample gave a positive signal, the comparable MW areas from the other mAb sample lane(s) were also excised and analyzed. A representative silver-stained gel with band samples removed is shown in Supplementary Data Figure S2. The samples were stored in 0.1% acetic acid and were analyzed by GeLC-MS/MS (Bioproximity, Chantilly, VA).

GeLC-MS/MS

A total of 248 numerically coded samples from 15 experiments were submitted for mass spectrometry analysis. The anti-PLP mAb experiments included analyses of proteins captured with F4.4C2 (n = 12), F3.9E9 (n = 7), P7.6A5 (n = 5), and F4.8A5, 2D2 and uncoated (PBS) bead samples (n = 2 each). The larger numbers of IP experiments and analyses performed with mAb F4.4C2 was a consequence of the larger numbers of visible bands in gels of eluates from beads coated with that mAb versus those with the other mAbs.

For identification of molecules that could contribute to PC12 cell neurite outgrowth inhibition, the mass spectrometry results from each experiment were screened for molecules captured by IP that might be bound by mAbs in live PC12 cells, that is cell membrane and ECM molecules. Initially, the search terms, "Neu," "adh," "myelin," "Eph," "Cdh," "MHC," "kinase," "receptor," "M6," and "CD" were used to identify potential candidate molecules. Additional screening for cell surface and ECM molecules of interest identified in eluates from mAb-coated beads was then performed for all experiments. Once identified in a single experiment, data from the other experiments were probed for the same molecules. Cell membrane and ECM molecules with known relevant neurodevelopmental functions were identified based on localization

and functional data for each in the Uniprot database (17). Sequence similarities of identified molecules with the PLP mAb epitopes were determined from BLAST searches (http://au.expasy.org/tools/blast/).

RESULTS

Myelin and Neuron Immunostaining in Human CNS Samples of Various Ages

We first analyzed the capacity of the mAbs to recognize myelin and other cells in the human CNS in samples from different developmental stages. With each of the anti-PLP mAbs (and consistent with previous studies of myelin proteins in human CNS development [18]), PLP immunoreactivity in myelin increased with age in fetal and postnatal samples and appeared complete in adult CNS samples (Fig. 2; Table 3).

In contrast, the patterns of neuronal recognition differed from those of developing CNS myelin. The anti-PLP 50–69 mAb F4.4C2, the anti-PLP 178–191 (P7.6A5) (both IgG$_{1\kappa}$), and anti-PLP 264–276 (P5.12A8, IgM) mAbs immunostained many neurons in multiple anatomic regions in the immature CNS samples (Figs. 3–5; Table 3). Neuronal immunostaining with these mAbs was greatest in samples from the third trimester of gestation; staining was decreased (Fig. 4; Supplementary Data Tables S6 and S7); neuronal immunostaining was essentially absent in other CNS regions in adult CNS samples (Supplementary Data Tables S3–S5, S8, and S9). The rat anti-PLP 264–276 mAb AA3 showed nearly identical myelin and neuronal immunostaining patterns to that of P5.12A8 (Supplementary Data Tables S3–S9; Table 3; and immunohistochemical data not shown). In contrast to F4.4C2, the anti-PLP 50–69 mAb F3.9E9 (IgG$_{2a\kappa}$) immunostained considerably fewer neurons whereas the 2 mAbs to the portion of PLP on the cytoplasmic face but not present in DM-20 (residues 116–150, i.e. 2D2 [IgG$_{1\kappa}$], to PLP 100–123, and 1C5 [IgG$_1$], to PLP

139–151), and the mAbs to PLP 200–219 (F4.8A5, IgG$_{1\kappa}$, second external loop of PLP) and MBP (IgG$_{1\kappa}$ and IgG$_{2a\kappa}$) did not immunostain CNS neurons in the FFPE tissue sections at any age despite immunostaining of CNS myelin and oligodendrocytes comparable to that of the other mAbs (Figs. 4 and 5; Supplementary Data Tables S3–S9).

A notable exception to this general pattern was the more frequent occurrence of immunostaining of pontine and medullary neurons (mostly of CN X nuclei) in adult samples (Fig. 4; Supplementary Data Tables S6 and S7). Other than in the brainstem, however, no clear patterns in the extent of neuronal immunostaining in the different anatomic regions studied among the mAbs could be identified. Together these data indicate that the expression of neuronal epitopes recognized by some anti-PLP mAbs is developmentally regulated and suggest that the epitopes recognized may have functional roles in immature neurons in addition to their roles in myelination by oligodendrocytes in the human CNS.

Anti-PLP mAbs Immunostain Cells in Adult NSCN

Despite the generally low extents of immunostaining of neurons in adult CNS samples (Figs. 4 and 5; Supplementary Data Tables S3–S9), some of the anti-PLP mAbs immunostained neuronal cells in FFPE samples of normal adult hippocampal dentate gyrus and olfactory bulb, that is NSCN (Fig. 6A, B; Table 3). This was particularly the case for mAbs that immunostained many neurons in early developmental CNS samples (Fig. 5). Specifically, the anti-PLP 50–69 mAb F4.4C2, the anti-PLP 178–191, and the anti-PLP 264–276 P5.12A8 consistently immunostained immature-appearing cells and cells with neuronal morphology in addition to myelinated axons in these regions. In contrast, the other anti-PLP 50–69 mAb F3.9E9 and mAbs to the PLP-specific region on the cytoplasmic face of PLP (i.e. 100–123 and 139–151
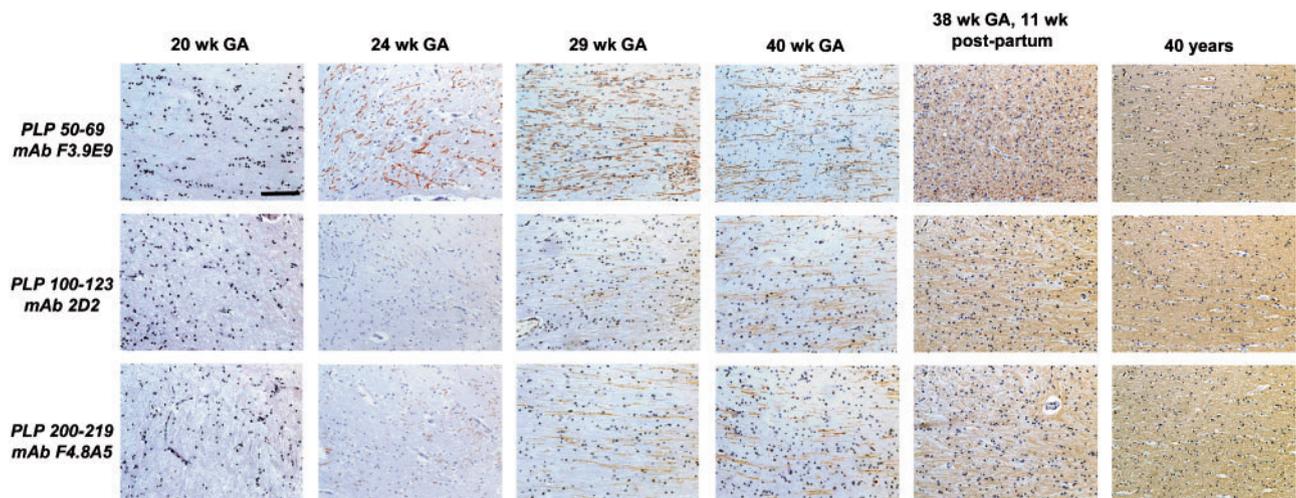

FIGURE 2. Immunoreactivities of 3 anti-PLP monoclonal antibodies in samples of human subcortical white matter from normal subjects of the indicated ages. There is increasing myelin immunostaining with increasing age. GA, gestational age; wk, weeks. Scale bar in upper panel = 100 μm, applies to all panels.

TABLE 3. Summary of Analyses of Anti-PLP and Anti-M6 mAb Tissue Immunohistochemistry

Monoclonal Antibody	mAb PLP Epitope	Increasing Immunostaining of CNS Myelin With Age*	Greater Immunostaining of Neurons in Normal Immature Versus Mature CNS Samples[†]	Neuronal Immunostaining in Human NSCN[‡]	Immunostaining of Intact Myelin and Myelin Debris in MS Patient Samples[§]	Axon Immunostaining in MS Lesions[§]
First external loop of PLP						
F4.4C2	50–69	+	+	+	+	+
F3.9E9	50–69	+	±	−	ND	ND
Cytoplasmic face of PLP						
2D2	100–123	+	−	−	+	−
1C5	139–151	+	−	ND	+	−
Second external loop of PLP						
P7.6A5	178–191	+	+	+	+	+
F4.8A5	200–219	+	−	+[¶]	+	±
C-terminus (cytoplasmic face of PLP)						
P5.12A8	264–276	+	+	+	+	−
AA3 (rat)	264–276	+	+	ND	ND	−
M6/GPM6b	NA	ND	ND	+[‖]	ND	ND

*See Figure 2.
[†]See Figures 3–5.
[‡]See Figure 6A, B.
[§]Supplementary Data Figures S3 and S4 and data not shown.
[¶]Olfactory bulb only.
[‖]See Figure 12A, B.
+, positive result; −, negative result; ±, equivocal result; MS, multiple sclerosis; NA, not applicable; ND, not done; NSCN, neural stem cell niches.
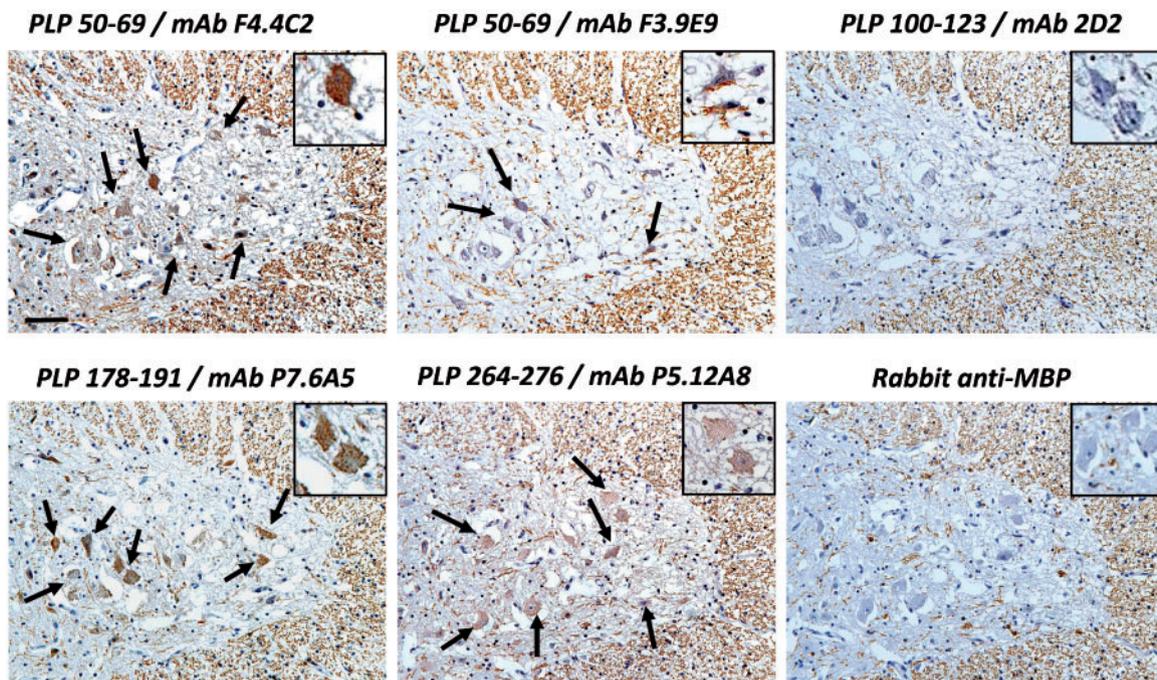

FIGURE 3. Immunoreactivity of anti-PLP monoclonal antibodies (mAbs) and anti-myelin basic protein (MBP) polyclonal Ab in spinal cord anterior horn samples of a normal 29-week gestational age infant. All mAbs immunostain white matter myelin (right side and on the periphery of gray matter in each panel). Anti-PLP 50–69 mAb F4.4C2, and the anti-PLP 178–191 and 264–276 mAbs immunostain the perinuclear cytoplasm of most of the anterior horn cell neurons (arrows). The anti-PLP 50–69 mAb F3.9E9 stains fewer neurons; anti-PLP 100–123 mAb 2D2 and anti-MBP Ab do not immunostain any neurons. Representative higher magnifications of anterior horn cells are shown in insets. Scale bar in upper panel = 100 μm and applies to all panels.
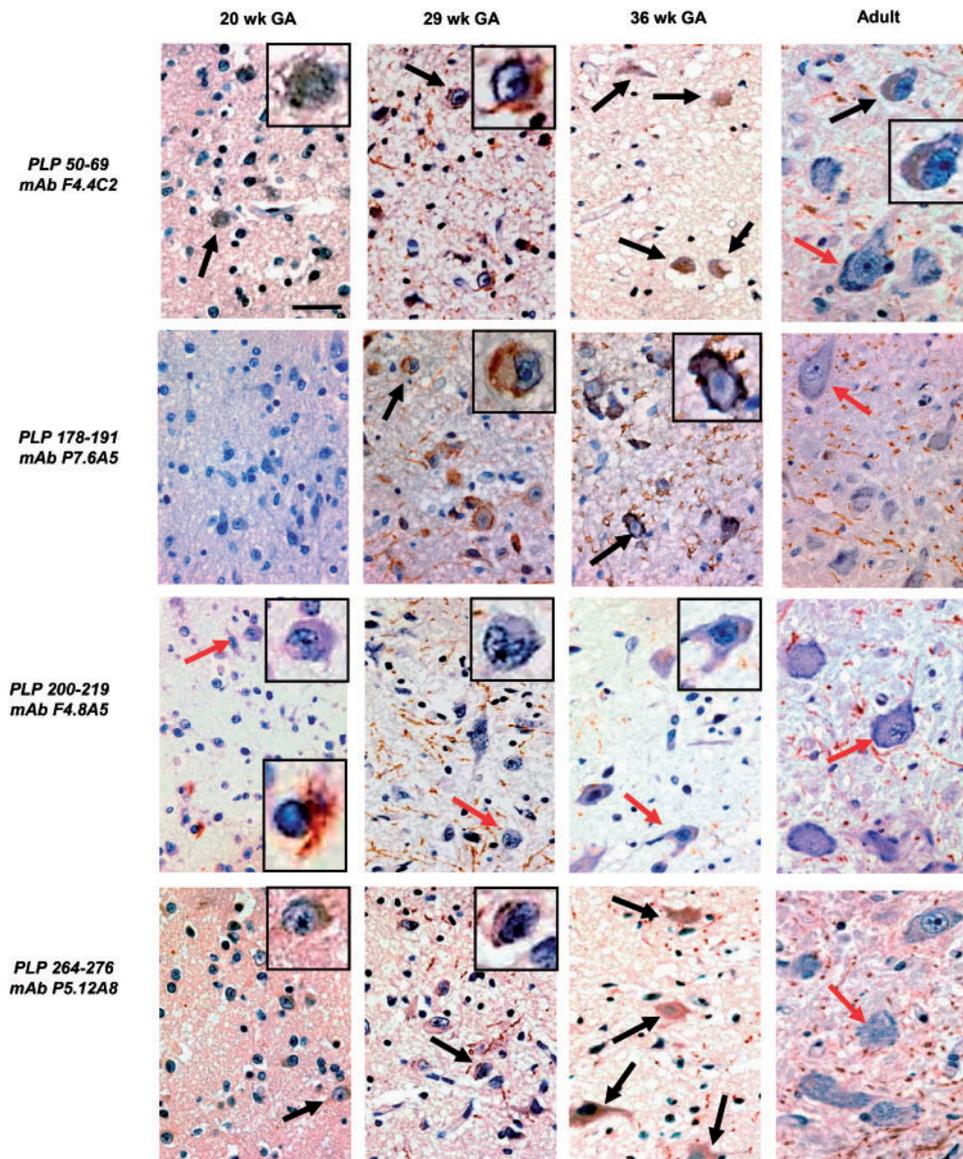
FIGURE 4. Immunoreactivity of anti-PLP monoclonal antibodies (mAbs) in normal human ventral medulla samples from subjects of different ages. Anti-PLP 50–69 mAb F4.4C2, anti-PLP 178–191 mAb P7.6A5, and anti-PLP 264–276 mAbs immunostain the perinuclear cytoplasm and cell surfaces of many neurons at early ages (black arrows) but to a lesser extent in the adult samples (red arrows). However, there is prominent neuronal staining of a neuron in the adult sample with mAb F4.4C2 (right upper corner). Adult samples were from subjects aged 55 and 58 years. The anti-PLP 200–219 mAb F4.8A5 did not immunostain neurons at any age (red arrows), although oligodendrocytes (lower inset at 20 weeks GA), and myelin at later ages are stained. Representative higher magnifications of stained and unstained neurons are shown in insets. GA, gestational age; wk, weeks. Scale bar in upper panel = 100 μm, applies to all panels.

[not shown]), and to MBP did not. The anti-PLP 200–219 mAb F4.8A5 immunostained some immature-appearing cells in the olfactory bulb (Fig. 6B), but showed less neuronal staining in the hippocampal dentate gyrus (Fig. 6A). No differences in immunostaining of NSCN could be identified among adult samples from patients of different ages and genders without or with neuropathological alterations (e.g. Alzheimer disease) in the NSCN (Supplementary Data Table S2C).

Anti-PLP mAb Immunostaining of Axons in Acute and Chronic MS Lesions

In FFPE sections of active and chronic inactive MS lesions, all of the anti-PLP mAbs tested immunostained myelin in adjacent normal-appearing white matter, residual myelin in lesions and granular extracellular, and phagocytosed myelin debris. In addition, the anti-PLP mAbs F4.4C2, P7.6A5, and F4.8A5 (to external face epitopes of PLP) immunostained
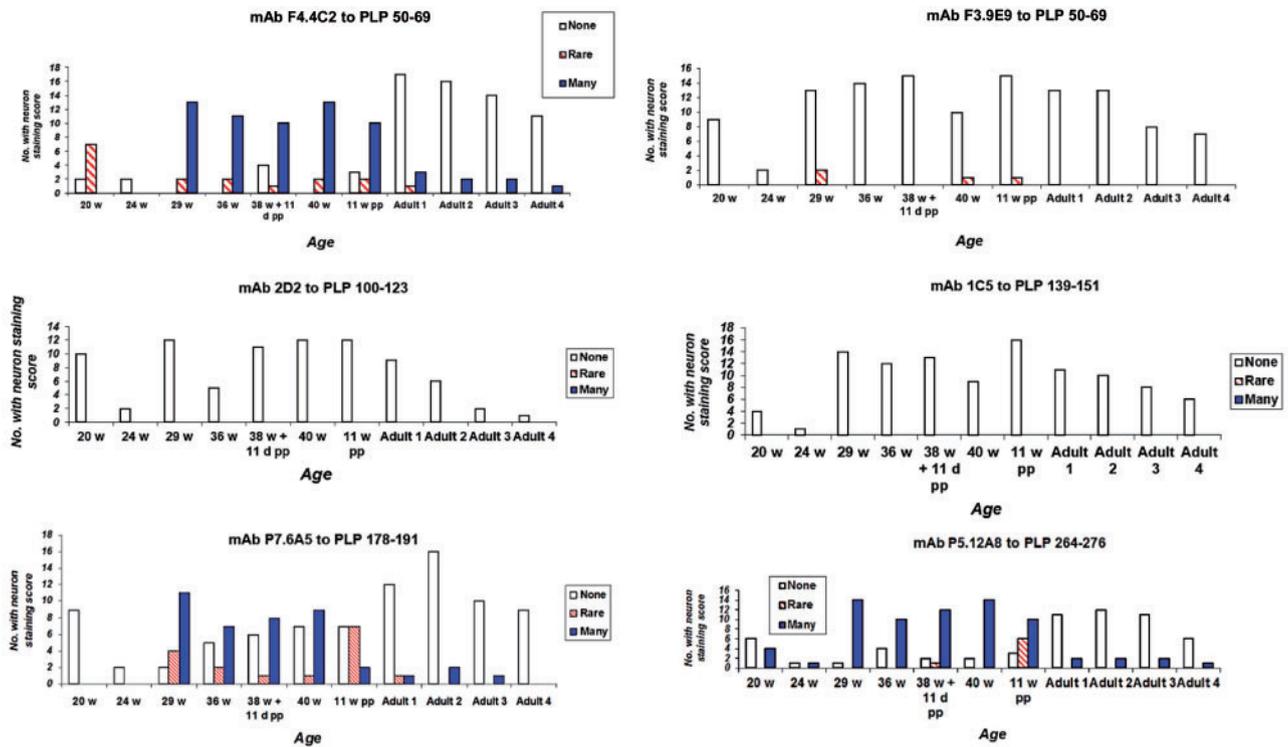
FIGURE 5. Summary of scores of neuron immunostaining with anti-PLP peptide monoclonal antibodies (mAbs) in normal human CNS tissue samples, (including cerebrum, deep gray matter, midbrain, pons, medulla, cerebellum, spinal cord), from subjects of different ages. Anti-PLP 50–69 mAb F4.4C2, anti-PLP 178–191 mAb P7.6A5, and the anti-PLP 264–276 mAb P5.12A8 showed maximal immunostaining in samples from the third trimester with less immunostaining in early ages and in adult samples. The anti-PLP 50–69 mAb F3.9E9 showed less immunostaining of neurons as compared to mAb F4.4C2. The 2 mAbs to the myelin proteolipid protein (PLP)-specific region, that is the region of PLP not present in DM-20, (residues 116–150), 2D2 (to PLP 100–123), and 1C5 (to PLP 139–151), did not immunostain neurons in any samples. The anti-PLP 200–219 mAb F4.8A5 and anti-MBP Abs also did not immunostain neurons at any age (not shown). Results for all mAbs in each CNS region analyzed are in Supplementary Data Tables S3–S9.

some elongated structures with smooth surfaces suggestive of axons in these lesions whereas the anti-PLP mAbs 2D2, P5.12A8, and AA3 (to cytoplasmic face PLP epitopes) did not immunostain these structures (Supplementary Data Figs. S3 and S4; Table 3).

Immune Recognition and Neurite Outgrowth Inhibition of RHPC In Vitro

To determine the potential pathogenetic significance of anti-PLP mAb recognition of immature neurons, we first investigated mAb effects on RHPC. Live cell staining of RHPC was tested by incubating the cells with the mAbs prior to fixation followed by immunoperoxidase staining for mouse Ig. The anti-PLP 50–69 mAbs F4.4C2 and F3.9E9, the anti-PLP 178–191 mAb P7.6A5, and the anti-PLP 200–219 mAb F4.8A5 immunostained the surfaces of some undifferentiated-appearing cells and neuronal processes. In contrast, the anti-PLP 100–123 mAb 2D2, and anti-PLP 139–151 mAb 1C5 (i.e. PLP-specific regions on the cytoplasmic face of PLP) and anti-PLP 264–276 (PLP cytoplasmic face, C-terminus), and PBS controls did not show

immunostaining of the surfaces of live RHPC (Supplementary Data Fig. S5; Table 4). Stains were performed on 2 different days of culture from days 1 to 7; results were consistent for each mAb on both days that they were tested. Similar results were obtained when the RHPC were fixed prior to immunostaining (data not shown).

We next determined the effects of the anti-PLP mAbs on RHPC neurite outgrowth; an anti-M6 mAb was used as a positive control for neurite outgrowth inhibition; the non-binding mAb 2D2 and antibody omission (PBS) were used as negative controls. In 3 experiments with each mAb, the 2 anti-50–69 mAbs and the anti-M6 mAb inhibited neurite outgrowth of E18 RHPC whereas the (non-binding) mAb 2D2 did not (Fig. 7A, B). In 1 of 2 experiments, the anti-178–191 mAb (P7.6A5) inhibited neurite outgrowth; in 1 experiment the anti-139–151 mAb 1C5 did not inhibit neurite outgrowth. In additional experiments, results with the other anti-PLP mAbs, including the (live cell-binding) anti-PLP 200–219 mAb F4.8A5 and the (live cell-non-binding) anti-PLP 264–276 mAb P5.12A8 (IgM), were inconsistent with respect to RHPC neurite outgrowth inhibition (data not shown).
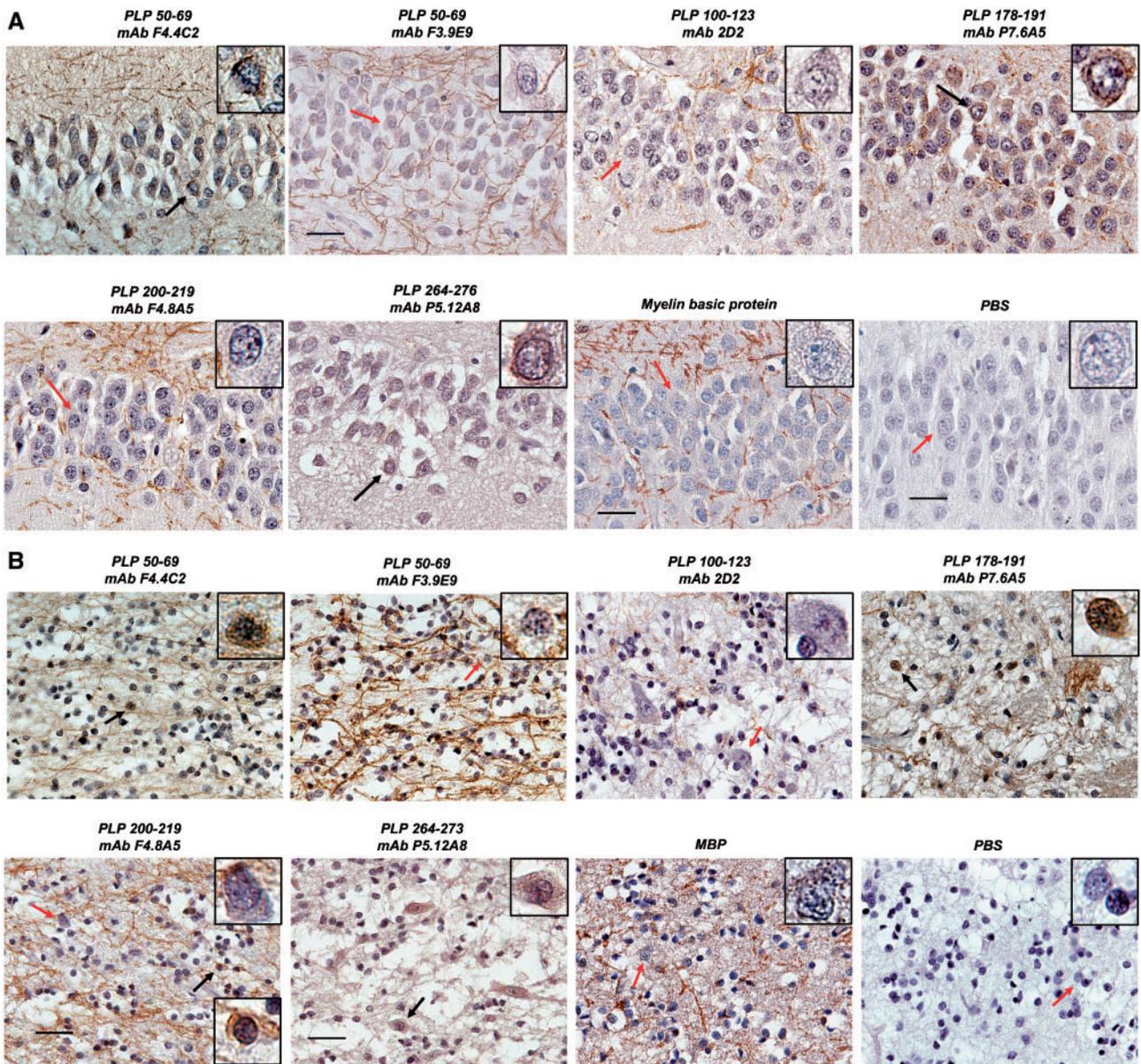
FIGURE 6. Immunostaining of adult human stem cell niches with anti-PLP monoclonal antibodies (mAbs). **(A)** Immunoreactivity of anti-PLP mAbs in samples of normal adult hippocampal dentate gyrus. The anti-PLP 50–69 mAb F4.4C2, the anti-PLP 178–191, and -PLP 264–276 mAbs immunostain myelinated fibers and cells with neuronal morphology (black arrows) whereas the anti-PLP 50–69 mAb F3.9E9, anti-PLP 100–123, and -200–219, and anti-MBP mAbs immunostain myelinated fibers but not neuron membranes or soma (red arrows). **(B)** Immunoreactivity of anti-PLP mAbs in samples of normal adult olfactory bulb. The anti-PLP 50–69 mAb F4.4C2, and the anti-PLP 178–191, and -264–273 mAbs immunostain myelinated fibers, cells with neuronal morphology, immature-appearing cells with round nuclei (black arrows), and the background neuropil. The anti-PLP 50–69 mAb F3.9E9, anti-PLP 100–123, and anti-MBP mAb immunostain myelinated fibers but predominantly do not immunostain immature or mature neuronal cells (red arrows). The anti-PLP 200–219 mAb F4.8A5 immunostains some immature-appearing cells (red arrow), but not more mature-appearing neurons (black arrow). Control samples with omission of primary mAb (PBS) show no immunoreactivity (red arrows in **A** and **B**). Scale bars = 25 μm and apply to all panels. All are immunoperoxidase with 3,3′-diaminobenzidine chromogen and hematoxylin counterstain. Representative higher magnifications of the stained and unstained neurons indicated by arrows are shown in insets.

Immune Recognition of PC12 Cells by Anti-PLP mAbs

It had previously been demonstrated that an anti-M6 mAb inhibited in vitro neurite outgrowth of the NGF-dependent PC12 cell line ([12]). This pheochromocytoma-derived cell line is a widely used as a model of neuronal differentiation ([19]). Importantly, these cells lack PLP mRNA and although DM-20 mRNA is present, it is reduced in NGF-treated

TABLE 4. Summary of Anti-PLP and Anti-M6 Monoclonal Antibody In Vitro Fixed and Live Cell Immunostaining, Neurite Outgrowth Inhibition, and Immunoprecipitation Analyses

Monoclonal Antibody	mAb PLP Epitope	RHPC Live Staining*	RHPC Neurite Outgrowth Inhibition†	PC12 Cell Fixed Staining‡	PC12 Cell Live Staining§	PC12 Cell Neurite Outgrowth Inhibition¶	IP Capture of Neuronal M6 Proteins‖	IP Capture of Cell Surface Neurodevelopmental Proteins Other Than M6 Proteins‖
First external loop of PLP								
F4.4C2	50–69	+	+	+	+	+	+	+
F3.9E9	50–69	+	+	+	+	+	+	+
Cytoplasmic face of PLP								
2D2	100–123‖‖‖	–	–	–	–	–	–	–‖‖
1C5	139–151‖‖‖	–	–	ND	–	ND	ND	ND
Second external loop of PLP								
P7.6A5	178–191	+	±	+	+	+	–	+
F4.8A5	200–219	+	±	ND	+	+	–	±‖‖
C-terminus of PLP (cytoplasmic face)								
P5.12A8	264–276	–	–	ND	–	ND	ND	ND
M6/GPM6b	NA	+	+	+	ND	+	ND	ND

*Supplementary Data Figure S5.
†See Figure 7A, B.
‡Supplementary Data Figures S6 and S7.
§See Figure 8.
¶See Figures 9A–C and 10.
‖See Figure 11.
‖‖Epitope within PLP-specific region, that is residues 116–150, Figure 1.
‖‖‖One protein captured, Figure 11.
+, positive result; –, negative result; ±, equivocal result; NA, not applicable; ND, not done; RHPC, E18 rat hippocampal precursor cells.

versus -untreated cells (20). Therefore, PC12 cells could be tested for direct effects of the anti-PLP mAbs on the differentiation of cells that do not express PLP. They could also subsequently be used as a bulk culture source for analyses of immune recognition of neurodevelopmental molecules by the mAbs without the presence of confounding non-neuronal populations.

In preliminary studies, we determined that both anti-PLP 50–69 mAbs and the mAb to the second extracellular loop (P7.6A5 [178–191]) immunostained cell cytoplasm, processes and neuronal growth cones of formalin-fixed NGF-treated PC12 cells whereas mAb 2D2 (PLP 100–123) did not (Supplementary Data Fig. S6). The PC12 cells and their processes were also immunostained with 2 Abs to M6b and 1 to neurofilament (Supplementary Data Fig. S7).

We then assessed whether the epitopes recognized by the anti-PLP mAbs are on external surfaces by immunostaining live PC12 cells. Both anti-PLP 50–69 mAbs, the anti-PLP 178–191 mAb P7.6A5, and the anti-PLP 200–219 mAb F4.8A5 immunostained cell surfaces and neurites of many cells (Fig. 8). Although there was cytoplasmic staining in the (subsequently fixed) cells, accentuated immunoperoxidase reaction product deposition was evident on cell surfaces (Fig. 8). In contrast, anti-PLP mAbs to epitopes on the cytoplasmic face of PLP (2D2 [PLP 100–123], 1C5 [PLP 139–151], and P5.12A8 [PLP 264–276]) did not stain the live cells (Fig. 8) (Table 4). These observations suggest that the mAb staining of live PC12 cells was due to recognition of external face rather than cytoplasmic face epitopes, that is the mAbs would not have access to the cytoplasm of live cells.

In addition to immunostaining observations in tissues (Figs. 3–5), and on live PC12 cells in vitro, pilot Western blot analyses using different chemical extraction protocols of PC12 proteins also indicated that immune recognition of anti-PLP 50–69 mAbs F4.4C2 and F3.9E9 differed but that they both are to hydrophobic integral membrane or membrane-associated protein epitopes (Supplementary Data Fig. S8).

Anti-PLP mAb Inhibition of PC12 Cell Neurite Outgrowth

We next tested effects of F4.4C2, F3.9E9, and P7.6A5 on NGF-induced PC12 cell differentiation in vitro using anti-M6 and 2D2 mAbs as positive and negative controls, respectively. The 2 anti-PLP 50–69 mAbs and the anti-178–191 mAb decreased the proportions of cells with neurite outgrowth and neurite lengths (Fig. 9A–C; Table 4). In separate experiments, the anti-PLP 200–219 mAb F4.8A5 also inhibited PC12 cell neurite outgrowth (Fig. 10). None of the inhibitory mAbs appeared to induce identifiable cytotoxic effects on the cells after brief (Fig. 8), or longer (Figs. 9A and 10) exposures. There was no reduction in cell numbers following mAb treatments up to 3 days and there was also no evidence of induction of apoptosis, as assessed in TUNEL and caspase-3 immunostains in the mAb-treated and control cultures (data not shown).
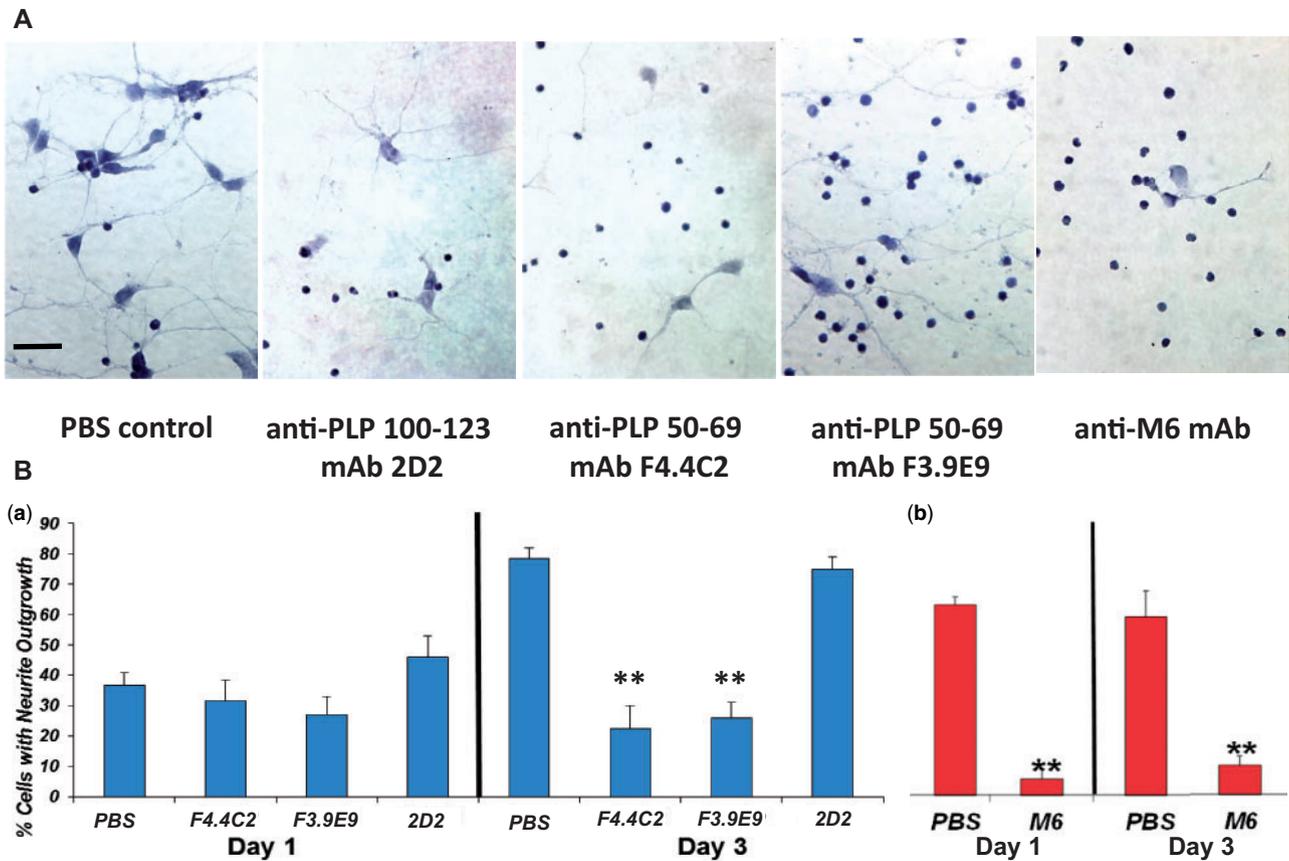
FIGURE 7. Effects of anti-PLP monoclonal antibodies (mAbs) on E18 rat hippocampal precursor cell in vitro neurite outgrowth. **(A)** Incubation with the anti-PLP 50–69 mAbs F4.4C2 and F3.9E9 and anti-M6 mAb resulted in larger proportions of immature-appearing round cells without neurite outgrowth or processes. Incubation with anti-PLP 100–123 mAb 2D2 did not result in inhibition of neurite outgrowth. Neurite outgrowth is also abundant on the cells in the PBS control well. Cells were grown on collagen-coated multiwell slides, fixed in formalin and counterstained with hematoxylin. (Day 3 in vitro results are shown). Bar = 25 μm, applies to all panels. Data are representative of 5 experiments with from 2 to 5 incubations for each mAb. **(B)** Representative data from 2 experiments showing effects of anti-PLP mAbs on rat hippocampal precursor cells. Proportions of cells with neurite outgrowth (defined by presence of cell processes equal to or greater than 6.25 μm), on the indicated day of incubation were determined in photographs of fields (day 1, n = 7 fields; day 3, n = 12 fields for each condition), of hematoxylin-stained fixed cells that had been incubated with the indicated mAbs or PBS **(a)**, or anti-M6 mAb or PBS **(b)**. Data were analyzed by 1-way ANOVA with Geisser-Greenhouse correction **(a)**, or Student t test **(b)**. **p < 0.001.

Identification of PC12 Cell Surface Proteins Captured by Anti-PLP mAbs in IP Experiments

A total of 41 903 proteins were identified in the band samples submitted for GeLC-MS/MS analysis in 15 experiments. These included samples from eluates from mAb-coated beads, uncoated bead eluates, cell pellets, pre-IP lysates, post-IP lysates, and mAb-coated bead eluates of molecules captured from lysates of NGF-untreated cells. In addition to cell membrane and ECM proteins, the molecules identified in most samples consisted of large numbers of cytoplasmic (e.g. filament proteins and enzymes), organelle and nuclear proteins. Based on the live cell staining and extraction data, we postulated that the molecules captured by the mAbs that were most relevant to the in vitro neurite outgrowth inhibition were ECM or integral membrane proteins with known neurodevelopmental functions that had been captured by and were eluted

from the mAb-coated beads. Examples of proteins identified in eluates from mAb-coated bead samples considered irrelevant to PC12 cell neurite outgrowth inhibition, (i.e. those not accessible to the mAbs in live cell cultures), in a representative experiment from mAb F4.4C2-coated bead eluates are listed in Supplementary Data Table S10. Plasma membrane proteins identified in that experiment that do not have known neurodevelopmental functions are listed in Supplementary Data Table S11.

Each mAb captured distinct but partially overlapping sets of neurodevelopmental cell surface and ECM proteins with potential relevance to neurite outgrowth inhibition (Fig. 11; Table 4). The 2 anti-PLP 50–69 mAbs F4.4C2 and F3.9E9 captured the same 11 cell surface and ECM proteins; these included the sequence-similar pgf neuronal glycoproteins M6a and M6b (boxed in Fig. 11), and 9 other proteins
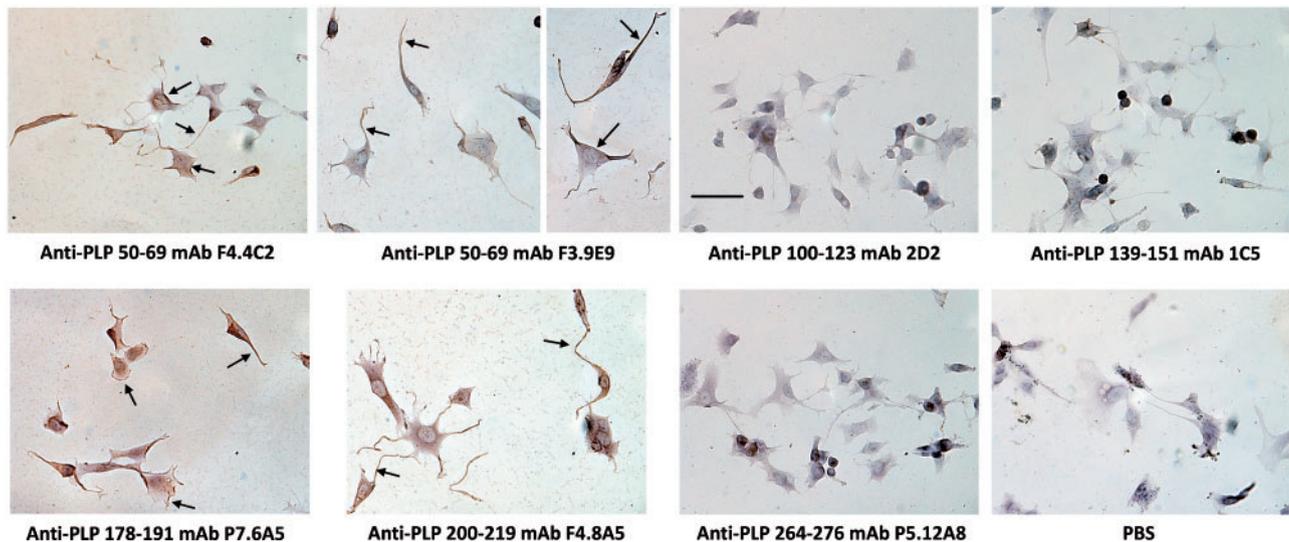
831

FIGURE 8. Live cell staining of NGF-treated PC12 cells incubated with the indicated monoclonal antibody (mAb) (5 µg/mL) or PBS for 2 hours prior to formalin fixation. After washing, the slides were immunostained for mouse Ig. The anti-PLP 50–69 mAbs (F4.4C2 and F3.9E9), the anti-PLP 178–191 mAb P7.6A5, and the anti-PLP 200–219 mAb F4.8A5 immunostain the cell body surfaces and neurites of many cells (arrows). The anti-PLP 100–123 mAb 2D2 and anti-PLP 139–151 mAb 1C5 (i.e. to myelin proteolipid protein [PLP]-specific regions), and the anti-PLP 264–276 mAb P5.12A8 (i.e. to an epitope on the cytoplasmic face of PLP), do not stain the live cells. A control with omission of primary mAb (PBS) also shows no immunoreactivity. All are immunoperoxidase for mouse Ig with 3,3'-diaminobenzidine chromogen and hematoxylin counterstain. Scale bar = 50 µm and applies to all panels.

with neurodevelopmental functions but without sequence similarity to PLP as determined by BLAST searches (Fig. 11, green text). The other 3 mAbs tested and the PBS-coated control beads did not capture M6a or M6b proteins. Five proteins were identified in eluates from beads coated with either anti-PLP 50–69 mAb or the anti-PLP 178–191 mAb P7.6A5 (2nd PLP loop) (Fig. 11, purple text). Five proteins were identified in eluates from beads coated with F4.4C2 and P7.6A5, but not F3.9E9 (Fig. 11, blue text). In 1 experiment, one of these proteins was also identified in a PBS control eluate. One protein was identified only in eluates from F4.4C2-, anti-PLP 200–219 mAb F4.8A5 (2nd PLP loop)-, and anti-PLP 100–123 mAb 2D2 (PLP-specific cytoplasmic region)-coated beads (1 experiment) (Fig. 11 red text). One protein was identified only in eluates from F3.9E9- and P7.6A5-coated beads (1 experiment) (Fig. 11, pink text).

Immunoprecipitated Neurodevelopmental Proteins Are Expressed in PC12 Cells and in Adult Human NSCN

To confirm the expression of the identified proteins, IHC was performed on fixed PC12 cells and adult human NSCN with commercial antibodies to M6b (gene, *Gpm6b*) (Table 1), and to other representative neuronal cell surface proteins (Table 2) that were immunoprecipitated by anti-PLP mAb F4.4C2. Neuronal glycoprotein M6b, EphA3, EphA10, EphB1, NrCAM, NCAM-1, and protocadherin-β12 (PCDHB12) were detected by IHC on cell surfaces and growth cones of fixed PC12 cells (Supplementary Data Fig. S9). In normal adult human hippocampal dentate gyri, there

was immunostaining for these proteins in perinuclear cytoplasm and cell surfaces of a subset of mature-appearing neuronal cells (Fig. 12A). In normal adult human olfactory bulb samples, there was immunostaining of perinuclear cytoplasm of a subset of cells with prominent membrane immunostaining for neuronal glycoprotein M6b, EphA3, EphB1, and PCDHB12 (Fig. 12B).

DISCUSSION

PLP is primarily a myelin structural protein but the *plp1* gene products, PLP and DM20 have additional roles in oligodendrocytes and neurons (21–24). Mutations of *plp1* cause the X-linked dysmyelinating disorders Pelizaeus-Merzbacher disease and spastic paraplegia type 2 in humans (25), and several recent studies have implicated *plp1* mutations in the pathogenesis of MS in some patients (26, 27). Although PLP sequences are identical among mammals and pgf proteins are highly conserved in all vertebrate species, little is known about neuronal expression, distribution, and functions of PLP epitopes or of other pgf proteins in the immature and mature human CNS and how they may relate to the pathogenesis of human CNS diseases.

Anti-PLP mAb Immunoreactivity at Different Ages in the Human CNS

We first surveyed archival normal tissue samples from patients of different pre- and postnatal ages and found that in addition to the expected increases in PLP immunoreactivity in myelin with age, immunostaining of CNS neurons with certain anti-PLP mAbs in the regions analyzed was considerable in
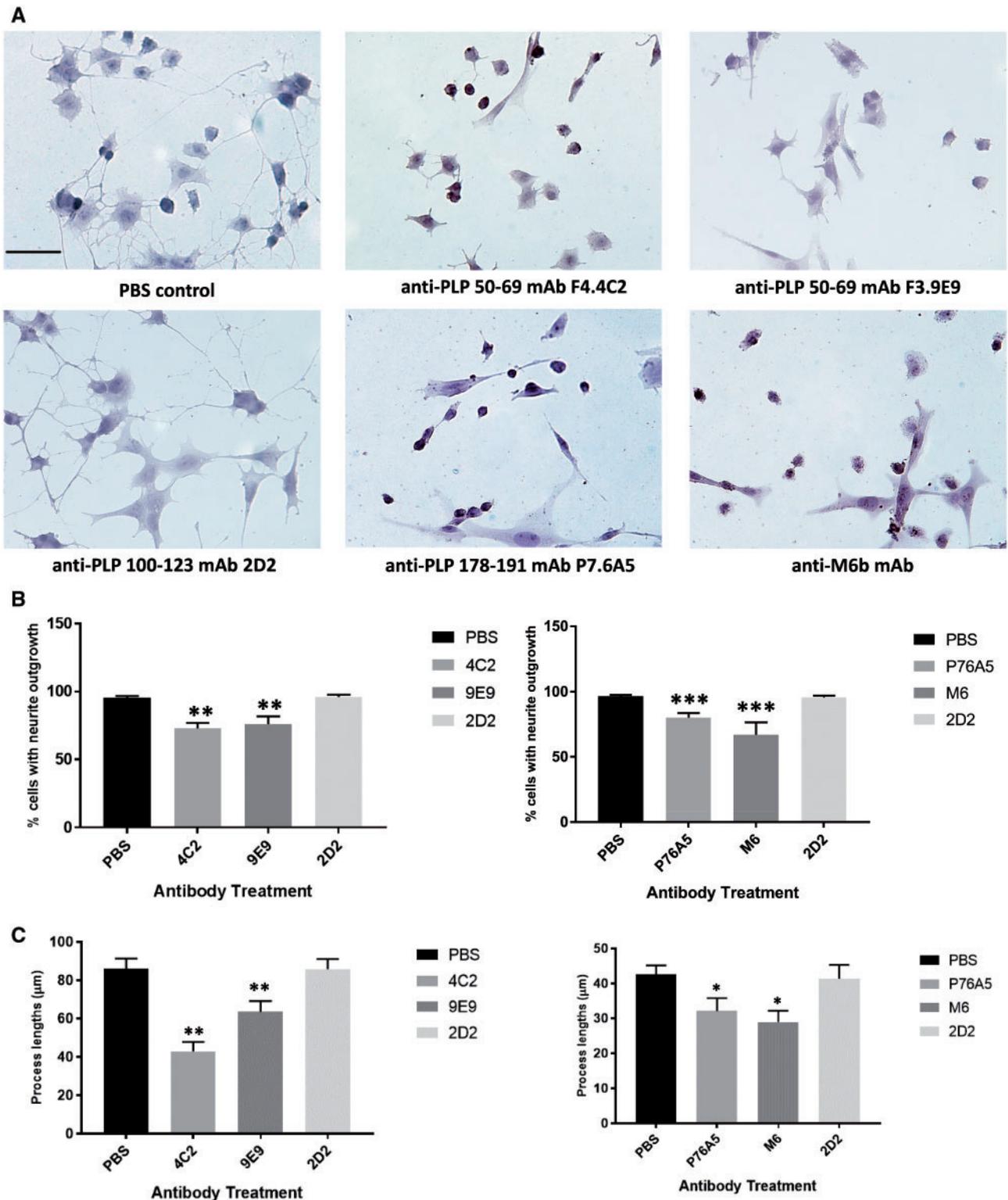
FIGURE 9. Effects of anti-PLP monoclonal antibodies (mAbs) (5 μg/mL) on PC12 cell in vitro neurite outgrowth. **(A)** Incubation with the anti-PLP 50–69 mAbs F4.C2 and F3.9E9, anti-PLP 178–191 mAb P7.6A5, anti-M6b mAb for 3 days resulted in larger proportions of immature cells (without neurite outgrowth or processes), whereas cultures incubated with anti-PLP 100–123 mAb 2D2 or PBS show normal neurite outgrowth with longer processes. Cells were grown on collagen-coated multiwell slides, fixed in formalin and counterstained with hematoxylin. Bar = 50 μm, applies to all panels. Data are representative of 7 experiments with 2–5 incubations for each condition. **(B, C)** Representative semiquantitative data (from 2 to 4 experiments for each mAb), showing effects of anti-PLP and -M6b mAbs on incidence of PC12 cell neurite outgrowth (defined by the presence of cell
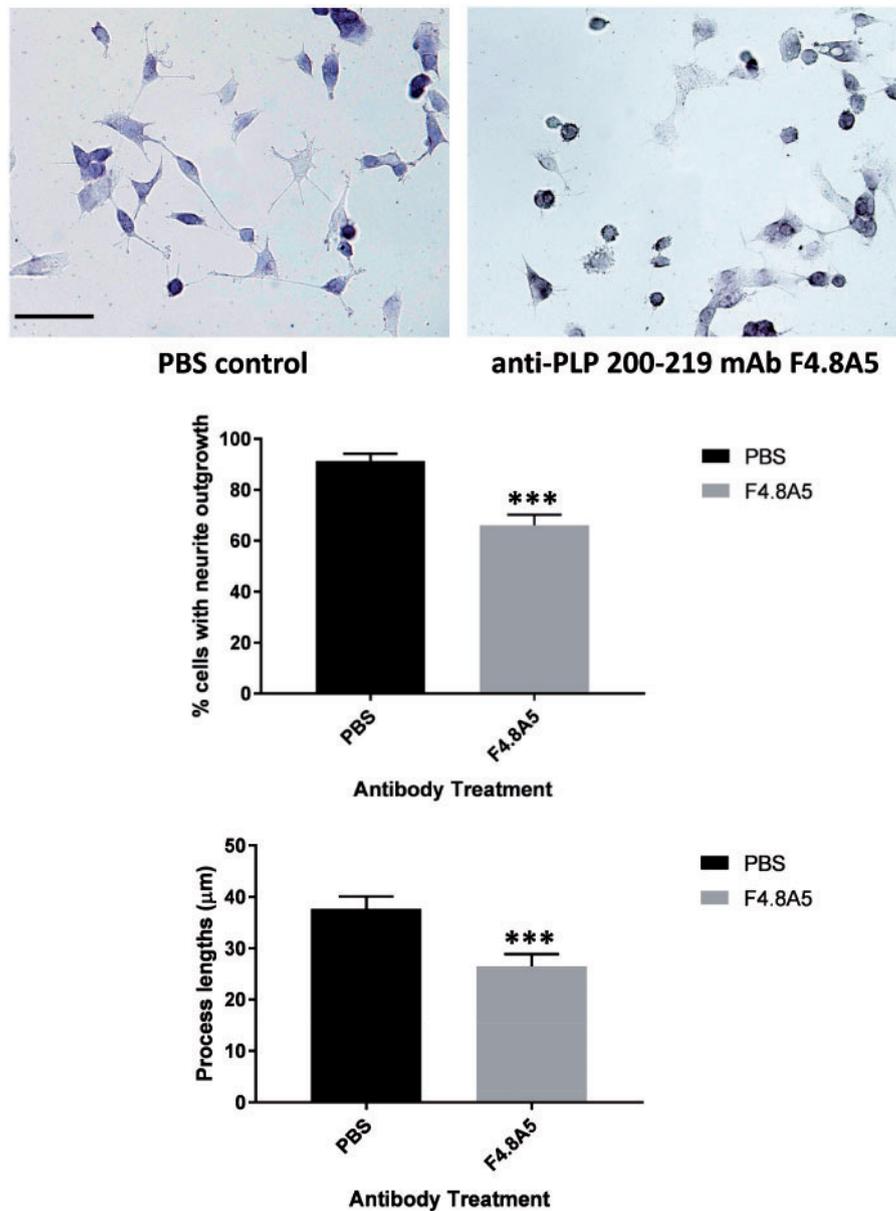
FIGURE 10. Effect of anti-PLP 200–219 monoclonal antibody F4.8A5 on PC12 cell neurite outgrowth. Upper panels show representative fields of control and F4.8A5-treated (5 μg/mL) cultures after 3 days in vitro. Bar = 50 μm, applies to both panels. The incidence of neurite outgrowth (middle panel, F4.8A5 vs PBS, ***p = 0.0002) and measurements of neuronal process lengths (lower panel, F4.8A5 vs PBS, ***p = 0.0014), were determined as in Figure 7. Data were analyzed with 2-tailed t test with Welch's corrections and are representative of 2 experiments.

FIGURE 9. Continued

processes equal to or greater than 3 nuclear diameters) **(B)** and neurite process lengths **(C)**. Proportions of cells with neurite outgrowth were determined in 10 fields of hematoxylin-counterstained fixed cells on day 3 of incubation with the indicated mAbs or PBS. For incidence of neurite outgrowth overall: **p < 0.001; ***p = 0.0002; paired comparisons for neurite outgrowth: PBS versus 9E9, p = 0.009; 4C2 versus 9E9, n.s. (not significant); PBS versus P76A5, p = 0.0003; PBS versus M6, p < 0.001; PBS versus 2D2, n.s. in both experiments (4C2 = F4.4C2; 9E9 = F3.9E9). For neurite process length measurements **(C)**, lengths of from 22 to 39 nonoverlapping processes in 10 fields per condition were measured. For overall process lengths: **p < 0.0001; *p = 0.0103; paired comparisons for process lengths: PBS versus 4C2, p < 0.0001; PBS versus 9E9, p = 0.0072; 4C2 versus 9E9, p = 0.0099; 2D2 versus 9E9, p = 0.0082; PBS versus P76A5, p = 0.0272; PBS versus M6, p = 0.022; PBS versus 2D2, n.s. in both experiments. Overall data were analyzed by 1-way ANOVA with Geisser-Greenhouse correction; paired comparisons were analyzed with 2-tailed t test with Welch's corrections.
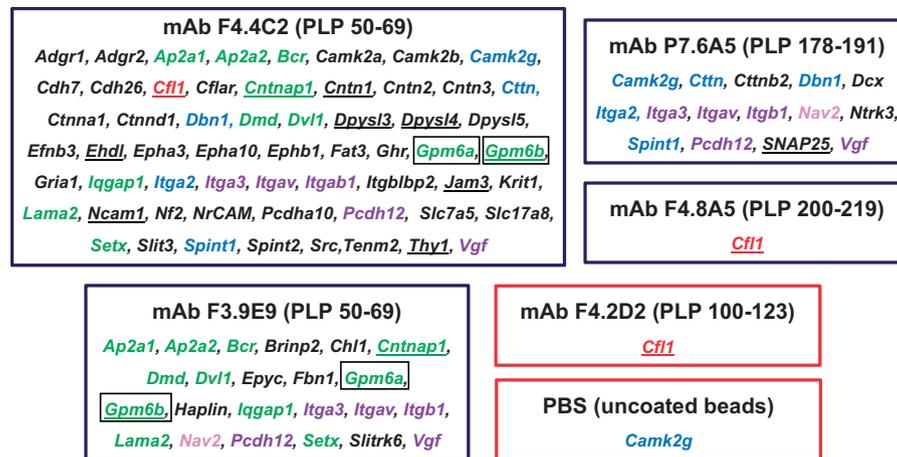
mAb F4.4C2 (PLP 50-69)

Adgr1, Adgr2, Ap2a1, Ap2a2, Bcr, Camk2a, Camk2b, Camk2g, Cdh7, Cdh26, Cfl1, Cflar, Cntnap1, Cntn1, Cntn2, Cntn3, Cttn, Ctnna1, Ctnnd1, Dbn1, Dmd, Dvl1, Dpysl3, Dpysl4, Dpysl5, Efnb3, Ehdl, Epha3, Epha10, Ephb1, Fat3, Ghr, Gpm6a, Gpm6b, Gria1, Iqgap1, Itga2, Itga3, Itgav, Itgab1, Itgblbp2, Jam3, Krit1, Lama2, Ncam1, Nf2, NrCAM, Pcdha10, Pcdh12, Slc7a5, Slc17a8, Setx, Slit3, Spint1, Spint2, Src, Tenm2, Thy1, Vgf

mAb P7.6A5 (PLP 178-191)

Camk2g, Cttn, Cttnb2, Dbn1, Dcx Itga2, Itga3, Itgav, Itgb1, Nav2, Ntrk3, Spint1, Pcdh12, SNAP25, Vgf

mAb F4.8A5 (PLP 200-219)

Cfl1

mAb F3.9E9 (PLP 50-69)

Ap2a1, Ap2a2, Bcr, Brinp2, Chl1, Cntnap1, Dmd, Dvl1, Epyc, Fbn1, Gpm6a, Gpm6b, Haplin, Iqgap1, Itga3, Itgav, Itgb1, Lama2, Nav2, Pcdh12, Setx, Slitrk6, Vgf

mAb F4.2D2 (PLP 100-123)

Cfl1

PBS (uncoated beads)

Camk2g

FIGURE 11. Cell-surface and extracellular matrix neuronal growth and differentiation molecules (listed by *gene*) identified by GeLC-MS/MS analysis of bands of eluates from the indicated anti-PLP monoclonal antibody (mAb)-coated and uncoated (PBS) control beads that had been incubated with NGF-treated and -untreated PC12 cell lysates. The large box groupings indicate the mAbs that did (black) and did not (red) inhibit in vitro PC12 cell neurite outgrowth. The 11 corresponding proteins in green text (AP-2 complex subunit α, AP-2 complex subunit α-2, [BCR, RhoGEF, and GTPase-activating protein], dystrophin, contactin-associated protein 1, segment polarity protein disheveled homolog DVL-1, neuronal membrane glycoproteins M6A and M6B, [IQ motif containing GTPase activating protein 1, Predicted, isoform CRA_b], laminin subunit α2 and senataxin), were identified in eluates from beads coated with both anti-PLP 50–69 mAbs F4.4C2 and F3.9E9 (1st PLP loop). *Gpm6a Gpm6b* are boxed to highlight that they are proteolipid gene family members and have sequence similarity with myelin proteolipid protein (PLP) 50–69. The 5 corresponding proteins in purple text, (integrin α3 variant A, integrin subunit αv, integrin β1, protocadherin 12, and neurosecretory protein VGF), were identified in eluates from beads coated with both anti-PLP 50–69 mAbs and anti-PLP 178–191 mAb P7.6A5 (2nd PLP loop). The 5 corresponding proteins in blue text (calcium-/calmodulin-dependent protein kinase type II subunit γ, Src substrate cortactin, drebin, integrin subunit α2, and Kunitz-type protease inhibitor 1), were identified in eluates from beads coated with F4.4C2 and P7.6A5; in 1 experiment, calcium-/calmodulin-dependent protein kinase type II subunit γ was identified in a PBS control eluate. *Cfl1* (cofilin-1, red text), was identified in eluates from F4.4C2-, anti-PLP 200–219 mAb F4.8A5 (2nd PLP loop), and anti-PLP 100–123 mAb 2D2 (PLP-specific cytoplasmic region)-coated beads (1 experiment each). *Nav2* (neuron navigator 2, pink text), was identified in eluates from F3.9E9- and P7.6A5-coated beads (1 experiment each). Underlined genes correspond to proteins identified as associated with CNS myelin (2).

the immature CNS tissues and, (except for the brainstem), generally decreased with age in most anatomic regions (Figs. 4 and 5; Supplementary Data Tables S3–S9; Table 3). This greater incidence of staining of neurons in adult brainstem parallels findings in rodents that indicate roles for neuronal PLP and other pgf protein expression in critical ventilatory control and response to acidosis (28–30).

In our analyses at the light microscopy level, PLP immunoreactivity was not limited to cell membranes, that is diffuse cytoplasmic immunostaining of neurons was often observed. This may relate to the use of postmortem FFPE specimens in which the cells are permeabilized following formalin fixation and tissue processing, other postmortem factors, and the use of antigen retrieval. However, in addition to membrane immunolocalization, soma-restricted *plp* gene products in neurons are characteristic of early development in other mammalian species (31). Therefore, the IHC staining likely represents true cytoplasmic localization of the epitopes in human CNS neurons. Together our observations indicate that there are distinct in situ patterns of neuronal PLP epitope expression over time that differ from those of PLP in myelin and suggest functional roles for the recognized epitopes in developing human neurons.

Anti-PLP mAb Immunoreactivity in Adult Human CNS NSCN

The extent to which neurogenesis in the CNS is preserved throughout life in healthy humans and the efficacy of endogenous neural stem cells for spontaneous restoration of brain function following injury in disease states and with aging are currently not understood (32–36). Because of the patterns of mAb neuronal immunorecognition in CNS samples of different ages and their potential relevance to neuroregeneration in the adult human CNS, we investigated anti-PLP mAb immunoreactivity in normal adult NSCN. We found that the anti-PLP mAbs that recognized neurons in immature human CNS samples also immunostained mature- and immature-appearing neuronal cells in adult human NSCN (Fig. 6A, B; Table 3). The NSCN immunostaining patterns of each mAb generally replicated the patterns in other CNS regions in immature CNS samples (Figs. 3–5; Supplementary Data Tables S3–S9). Specifically, the anti-PLP 50–69 mAb F4.4C2 (IgG1$_{1κ}$) consistently immunostained numerous neuronal cells in the NSCN whereas the anti-PLP 50–69 mAb F3.9E9 (IgG$_{2aκ}$) did not. The isotype difference between these mAbs could be 1 factor contributing to these differences, which were also evident in the different age samples (Fig. 5; Table 3).
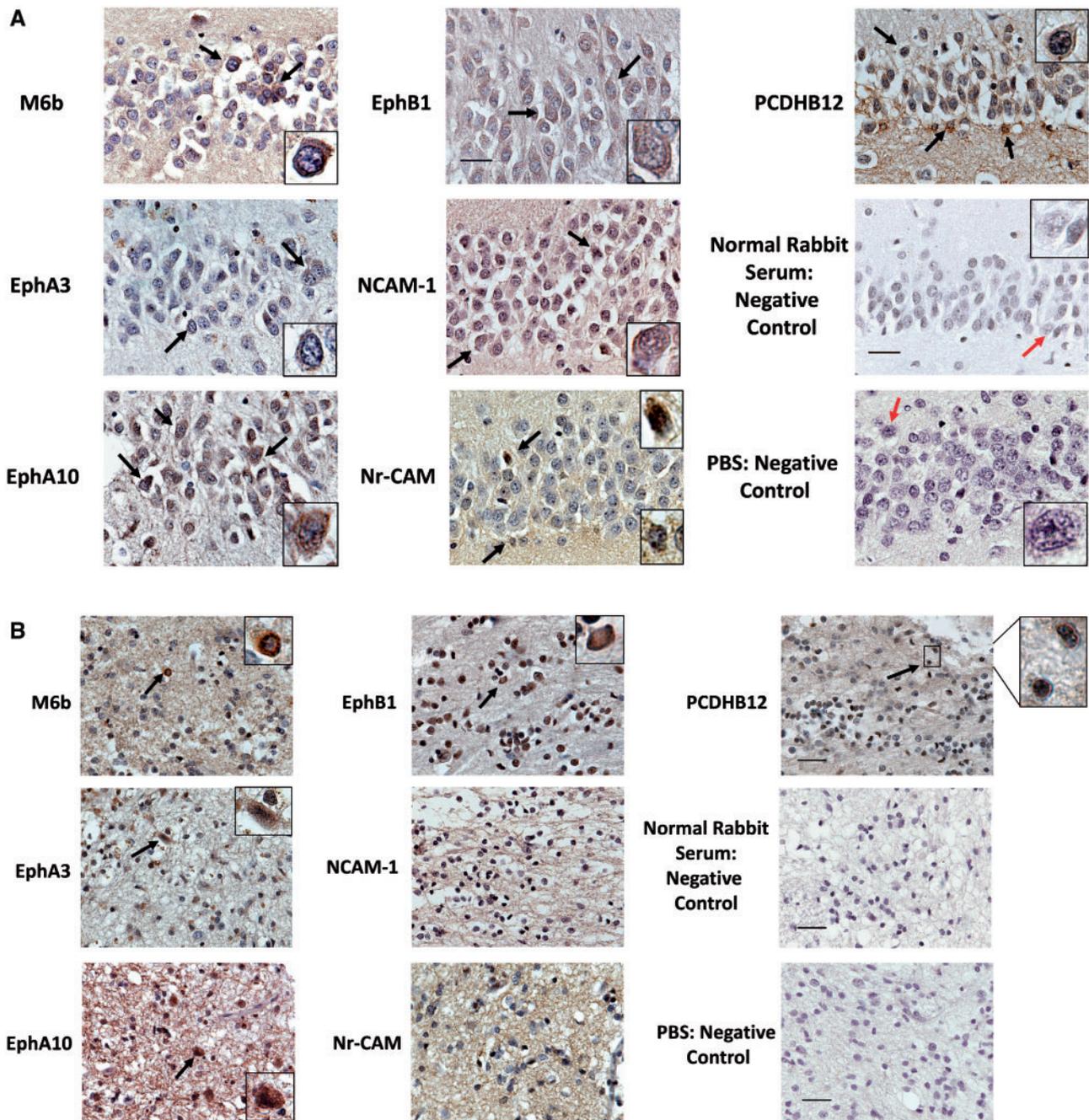
FIGURE 12. Representative PC12 cell proteins immunoprecipitated by anti-PLP monoclonal antibody (mAb) F4.4C2 in IP experiments are expressed in adult human neural stem cell niches (NSCN). Immunostaining of adult human NSCN was performed with commercial antibodies to neuronal glycoprotein M6b (gene, *Gpm6b*) (Table 1), and to other neuronal cell surface proteins (Table 2). **(A)** Immunoreactivity in samples of normal adult hippocampal dentate gyrus. Most fields show immunostaining of perinuclear cytoplasm of a subset of mature-appearing neuronal cells (black arrows). There is strong cell surface immunostaining seen for EphB1 (*EphB1*), NCAM-1 (*Ncam1*), and protocadherin β12 (PCDHB12, *Pcdh12*). Control samples with normal rabbit serum or omission of primary mAb (PBS) show no immunostaining of neuronal cells (red arrows). **(B)** Immunoreactivity in samples of normal adult human olfactory bulb. Most fields show immunostaining of perinuclear cytoplasm of a subset of neuronal cells (black arrows). There is strong cell surface immunostaining seen for neuronal glycoprotein M6b, EphA3 (*Epha3*), and protocadherin β12 (PCDHB12). Immunostaining for NCAM-1 and Nr-CAM (*NrCAM*) resulted in staining of background neuropil only in the olfactory bulbs. Control samples with normal rabbit serum or omission of primary mAb (PBS) show no immunostaining of neuronal cells. Representative higher magnifications of stained and unstained neurons are shown in insets and in an adjacent panel for PCDHB12 in **(B)**. Scale bars = 25 μm and apply to all panels. All are immunoperoxidase with 3,3′-diaminobenzidine chromogen and hematoxylin counterstain.

The anti-PLP 178–191 mAb P7.6A5 also immunostained many neuronal cells in NSCN whereas the immunostaining with anti-PLP 200–219 mAb F4.8A5 was less consistent. Both are IgG$_{1\kappa}$ and both are against second external loop PLP epitopes. As in the immature human CNS tissues, the anti-PLP 264–276 mAb P5.12A8 (IgM) also consistently immunostained neuronal cells in NSCN. In contrast, the mAbs to the PLP-specific regions (PLP 100–123 and 139–151, both IgG$_{1\kappa}$), and to MBP, (which is also on the cytoplasmic face of myelin), did not immunostain neuronal cells in NSCN despite comparable immunostaining of myelinated axons in all cases (Figs. 2–4). These latter findings with identical mAb isotypes support the specificity and selectivity of neuronal immunostaining results in FFPE samples and suggest that the epitopes recognized by the individual mAbs in neurons may have functional roles throughout the human lifespan.

Live Staining and Neurite Outgrowth Inhibition of RHPC

We postulated that the anti-PLP antibodies that immunostained immature neurons and neurons in adult NSCN would inhibit in vitro neurite outgrowth through their recognition of M6 or other related pgf proteins. For RHPC neurite outgrowth inhibition experiments, the mAb concentrations (10 μg/mL) were as originally used by Lagenaur et al (9). In contrast to the divergent results in immunostaining of FFPE sections, both anti-50–69 mAbs immunostained the surfaces of live RHPC cells (Supplementary Data Fig. S5), and consistently inhibited neurite outgrowth (Fig. 7A, B; Table 4). In contrast, although the mAbs to the second external loop of PLP (178–191 and 200–219) immunostained surfaces of live RHPC (Supplementary Data Fig. S5), neurite outgrowth results with these mAbs on RHPC were inconsistent. The mAbs to the PLP cytoplasmic face epitopes (100–123, 139–151, and 264–276) did not immunostain live RHPC or inhibit their neurite outgrowth (Supplementary Data Fig. S5 and data not shown; Table 4). These latter observations support the specificity of staining and neurite outgrowth inhibition results with the mAbs to the first external loop epitope. They also suggest that the epitope(s) recognized by those mAbs would not be accessible on live cells in RHPC cultures and that this might account for their failure to inhibit neurite outgrowth.

Because PLP, M6 proteins and other pgf proteins can be expressed on both glial and neuronal cells, it was not possible to identify effects of the mAbs on neurons versus non-neuronal cells in the mixed lineage populations of RHPC cultures. Multiple direct and indirect effects on different populations might have contributed to some of the inconsistent findings of RHPC neurite outgrowth inhibition by the mAbs to the second external loop (Table 4).

Live Staining and Neurite Outgrowth Inhibition of PC12 Cells

To overcome the problem of multiple cell populations in RHPC cultures, we analyzed PC12 cells and found that the combined live staining and neurite outgrowth inhibition results with the cell line were more congruent for each mAb, that is F3.9E9, F4.4C2, P7.6A5, and F4.8A5 all immunostained live PC12 cells, consistent with recognition of epitopes on their external surfaces and each inhibited neurite outgrowth (Figs. 8–10; Table 4). As with RHPC, the mAbs to epitopes on the cytoplasmic face, (PLP 100–123 and 139–151), did not immunostain live PC12 cells; when tested repeatedly as a negative isotype-matched control, the anti-PLP 100–123 mAb 2D2 also did not inhibit PC12 cell neurite outgrowth (Fig. 9A–C). The anti-264–276 mAb P512.A8 (IgM) was not investigated for neurite outgrowth inhibition of PC12 cells because it did not inhibit neurite outgrowth of RHPC and did not stain live PC12 cells (Fig. 8; Table 4).

PC12 Cell Neurodevelopmental Proteins Immunoprecipitated by Anti-PLP mAbs

To characterize possible mechanisms for the neurite outgrowth inhibition, we performed IP analyses to identify potential anti-PLP mAb target molecules on PC12 cells. Large numbers of plasma membrane and non-membrane proteins were captured from PC12 cell lysates by mAb-coated beads and identified in the bead eluates (Supplementary Data Tables S10 and S11). Based on the live-staining results, we focused on rat cell membrane and ECM proteins with known neurodevelopmental functions that were captured by and eluted from the mAb-coated beads and therefore could have contributed to neurite outgrowth inhibition by the anti-PLP external face mAbs (Fig. 11).

Three of the 4 mAbs that immunostained live PC12 cells and inhibited neurite outgrowth (F4.4C2, F3.9E9, and P7.6A5) captured distinct but partially overlapping groups of neurodevelopmental proteins. Because in our previous study of nonhuman vertebrate tissues, sequence similarities between PLP peptide epitopes 50–69 and 178–191 and neuronal pgf proteins (M6a, M6b, Rhombex-29) correlated with the extent of neuronal immunostaining (Supplementary Data in [3]), we postulated that the neurite outgrowth-inhibiting mAbs would cross-react with and capture sequence-similar epitopes of pgf proteins expressed by the PC12 cells. Indeed, the anti-50–69 mAbs F4.4C2 and F3.9E9 captured the pgf M6a and M6b neuronal proteins, consistent with the notion that sequence similarity played a part in the mAb live cell immunostaining, IP capture and in vitro neurite outgrowth inhibition for those mAbs (Table 4). The potential recognition of M6 proteins by these anti-PLP mAbs on PC12 cell surfaces suggests that the mechanisms of neurite outgrowth inhibition may be similar to those of the anti-M6 mAb, that is suppression of NGF-triggered Ca^{2+} influx (12).

The PLP cytoplasmic face mAb epitopes have sequence identities with the M6 proteins, (particularly with gpM6b), that are comparable to that of the 50–69 epitope (Supplementary Data Table S12). This supports the notion that for the mAbs to 100–123 and 139–151, accessibility to cytoplasmic face epitopes may have been a limiting factor for neuronal immunostaining and neurite outgrowth inhibition. However, the anti-PLP 178–191 mAb P7.6A5 also immunostained neurons, inhibited neurite outgrowth and has a comparable level of sequence similarity with M6 proteins (Supplementary

837

Data Table S12), but it did not capture M6 proteins. Thus, sequence similarities between PLP mAb epitopes and M6 proteins could not account for the PC12 cell neurite outgrowth inhibition results for all of the mAbs.

The anti-PLP 200–219 mAb F4.8A5 inhibited PC12 cell neurite outgrowth but it displayed a distinct profile as follows: (i) It did not immunostain any neurons in the nonhuman vertebrate tissue samples, even when there was considerable sequence similarity between PLP peptide 200–219 and known neuronal proteins of the tested nonhuman vertebrate species (Supplementary Data in [3]). (ii) It did not immunostain neurons in human CNS dentate gyrus and it immunostained fewer neurons in the olfactory bulb than the other neurite outgrowth-inhibiting mAbs (Fig. 6A, B). (iii) It only captured 1 protein (cofilin-1 [*Cfl1*]), (which was also captured by F4.4C2 and the non-inhibiting, nonbinding mAb 2D2), in IP experiments (Fig. 11). The second external loop of PLP contains cysteine residues and the comparable region in gpM6a is critical for rat hippocampal cell filopodium outgrowth and synaptogenesis (37). How these cysteine residues in the second loop epitopes might have affected the recognition by P7.6A5 and F4.8A5 with respect to conformations in FFPE tissues, in vitro and in the IP analyses, are unclear.

Our inability to identify possible target molecules for F4.8A5 despite the finding that the F4.8A5 epitope has also a high sequence similarity with gpM6b (Supplementary Data Table S12), and that it immunostained some neuronal cells and inhibited neurite outgrowth highlights limitations of the IP experiments and their interpretation. The samples submitted for analysis were selected and cut from the gels based on visualization of bands; variations in numbers of samples submitted for analysis for each mAb, (i.e. most numerous for F4.4C2), likely contributed to disparate numbers of captured proteins identified for each mAb. Additional proteins not captured by the mAb-coated beads or not eluted from them may not have been detected or identified by GeLC-MS/MS because they could have undergone degeneration or conformational changes at various steps in the procedure (e.g. protein extraction, coating of the beads, IP, elution); or their epitopes might have been blocked by other proteins.

Many other neuronal and myelin membrane proteins without sequence similarities with PLP were also eluted from beads coated with the neurite outgrowth-inhibiting mAbs (Fig. 11). Some non-pgf proteins were captured by either F3.9E9 or F4.4C2 and P7.6A5; some (i.e. integrins, PCDH12 and neurosecretory protein VGF) were captured by all 3 of these mAbs despite their different specificities (50–69 vs 178–191). Because the proteins captured by 1 or more of the mAbs and identified in the IP experiments may be binding partners of the molecules recognized by the mAbs rather than being bound directly by the mAbs, some of them may not be relevant to or sufficient for neurite outgrowth inhibition. For example, the calcium-/calmodulin-dependent protein kinase type II subunit γ [*Camk2g*], was captured by PBS-coated beads as well as F4.4C2 and F3.9E9 (Fig. 11). The extent of IP capture by the negative control 2D2- and PBS-coated beads was, however, minimal as compared to the multiplicity of molecules captured by the neurite outgrowth-inhibiting mAbs (other than F4.8A5). Furthermore, the neurodevelopmental functions of

some of the identified proteins not included in Figure 11 may not be currently known and relevant molecules could have been excluded. Importantly, IP capture and identification in mAb-coated bead eluates argues for but does not prove binding in situ, in vitro or in vivo. Further studies would be necessary to prove that direct binding of each of the proteins identified occurs in the absence of many other confounding factors.

In view of these considerations, the IP results cannot be regarded as definitive identification of all molecules relevant to anti-PLP mAb in vitro neurite outgrowth inhibition. The analyses do indicate that: (i) there is the potential for binding to numerous cell surface neurodevelopmental molecules expressed by PC12 cells by each neurite outgrowth-inhibiting anti-PLP mAb; (ii) the binding of an individual mAb to each PLP epitope may be distinct but may not predict specific pathobiological consequences of a polyclonal Ab response; and (iii) sequence identity to M6 proteins is only 1 potential determinant of the effects of an individual mAb. The independent IHC results demonstrating several of the captured molecules in human NSCN (Fig. 12A, B), indicate the potential relevance to human neuronal precursor cell differentiation in vivo.

Antibody Multispecificity

Both specificity of epitope recognition and promiscuity, that is binding to a variety of different and structurally unrelated self and non-self (foreign) antigens by a single antibody, are intrinsic, evolutionarily conserved characteristics of vertebrate antibodies (38–40). As suggested by James et al, multi-specific recognition may increase the potential for the development of pathogenic autoimmunity (41, 42). Our IP data suggest that in vitro neurite outgrowth inhibitory effects were due to mAb binding to epitopes of multiple cell surface neurodevelopmental molecules, thereby providing support for this concept. Although the structural relationships underlying mAb recognition and functional interactions of the identified molecules in vitro and in vivo are not known at this time, any of the positive "hits" from the IP studies can be considered a potential specific target of the mAbs. The close physical proximity of membrane molecules with portions on external surfaces might facilitate the hydrogen bonds that permit promiscuous Ab recognition (43). Furthermore, because neuronal precursor cells undergo rapid growth and differentiation, the critical neurodevelopmental membrane molecules are highly expressed and, therefore, would more likely to have been bound to the anti-PLP mAbs in the in vitro models.

Anti-PLP Abs in Patients With Chronic MS

Leptomeningeal B cell aggregates are considered the sources of pathogenic Abs and the drivers of immunopathology in chronic CNS autoimmune diseases, particularly MS (44). Many previous studies have demonstrated that some but not all MS patients have increased anti-PLP Abs in their sera and CSF as compared to controls; in some of these studies, the detected antibody levels have correlated with evidence of clinical disease activity and some have included Abs to native or

mutant peptide epitopes in regions of the PLP molecule corresponding to the epitopes of our mAb panel (45–58). However, the methods for characterizing the Ab responses (e.g. immunofluorescence staining of tissue or tissue slices, ELISA, and antigen arrays), and the specific epitopes analyzed in these studies are highly heterogenous and most have not systematically and comprehensively focused on peptide sequences encompassing multiple regions of the PLP molecule. Studies of in situ staining of CNS tissues with MS patient biofluid samples have also not examined human or nonhuman NSCN. The patient samples analyzed (serum vs CSF, pediatric vs adult MS, other demyelinating diseases, etc.), and the types and numbers of healthy and other neurological diseases patient controls among these studies are also highly variable making direct comparisons difficult. Therefore, despite the well-known frequent presence of oligoclonal bands in the CSF in MS patients, it is not surprising that there is no consensus on the pathogenetic significance of anti-PLP Abs or, indeed, of Ab responses to any single antigen in MS patients.

Implications for Remyelination, Neuronal Injury, and Disease Progression in Chronic MS Patients

Despite current therapies, chronic MS patients typically exhibit clinical and neuroimaging disease worsening over time. The pathogenetic mechanisms underlying this progression are not understood (59). As expected, none of the anti-PLP mAbs immunoprecipitated PLP or DM-20 from PC12 cells and none of the mAbs captured other major myelin proteins such as MBP. However, some of the other captured cell membrane and ECM neurodevelopmental proteins function in myelination or are also expressed in CNS myelin (underlined in Fig. 11) (2). The potential immunorecognition of those molecules and others involved in myelination, for example ephrin B3 (*Efnb3*) and α2 laminin subunit (*Lama2*), (captured by F4.4C2), and αv integrin (*Itgav*), (captured by 3 mAbs), might also affect remyelination of demyelinated lesions in MS patients (23, 60–62).

To address this issue, we undertook a limited immuno-histochemical analysis of MS lesions and determined that the anti-PLP external face mAbs F4.4C2, P7.6A5, and F4.8A5 immunostained some individual apparently demyelinated and dystrophic axons as well as residual and phagocytosed myelin in active and chronic inactive lesions; the anti-PLP cytoplasmic face mAbs 2D2, P5.12A8, and AA3 only immunostained myelin (Supplementary Data Figs. S3 and S4; Table 4). However, it is not known if neurite outgrowth inhibition within MS lesions could in part be attributable to Ab-mediated effects on neuronal precursor cells. Separating the Ab effects on myelin and remyelination from effects on neurons and neuronal precursor cells would be difficult.

The PC12 cell surface molecules that were captured by the anti-PLP mAbs, (e.g. NCAM-1, protocadherins, contactins, and ephrins/Ephs), are expressed by non-myelin-producing cells and Abs to them have also been implicated in MS pathogenesis (51, 56, 63–70). Hippocampal and olfactory bulb atrophy identified both in imaging and neuropathological studies have also been suggested as the bases for impaired olfaction, memory loss, and cognitive

decline in MS patients (71–74). Whether these focal anatomic abnormalities are consequences of more general pathogenetic mechanisms of MS or indicate specific targeting in these regions by autoantibodies or other mechanisms is not known. In this regard, Oreja-Guevara et al demonstrated reduction of expression of stem cell and mitosis markers in NSCN in a patient with acute fulminant MS (Marburg form), suggesting that neurogenesis was inhibited in early disease stages in that patient (75). Similarly, in myelin oligodendrocyte glycoprotein (MOG)-induced acute experimental autoimmune encephalomyelitis, (in which myelin breakdown may result in the generation of anti-PLP Abs [58]), Kesidou et al identified serum antibody binding to neural precursor cells; those authors emphasized the potential for impaired remyelination rather than impaired neuroregeneration (76).

It is notable that in addition to the general lack of immunoreactivity of the mAbs in adult CNS neurons, there was almost no overlap of molecules captured by the anti-PLP mAbs with antigens found on mature neurons that are associated with paraneoplastic autoimmune encephalitides (77) (Supplementary Data Table S11). This suggests that anti-PLP Abs comparable to the mAbs studied could have effects on function and/or regeneration of neuronal precursor cells or immature rather than mature neurons in the human CNS and that clinical progression and focal atrophy might in part be attributable to autoantibody-mediated inhibition of neuronal regeneration in specific anatomic regions including NSCN in chronic MS patients.

Potential Implications for Impaired Neuroregeneration in Tissue Destructive Lesions, Aging and Other Neurological and Psychiatric Conditions

In addition to human demyelinating diseases, B cell infiltrates and autoantibody responses have been implicated in the pathogenesis of progressive functional impairment after CNS destructive lesions, including spinal cord and brain trauma (78–80), and infarcts (81, 82). Autoantibodies have also been suggested to contribute to chronic human neurodegenerative conditions in which there is secondary demyelination, that is following neuronal injury or degeneration. These include those occurring in aging (83) and Alzheimer disease (84). In this regard for example, P7.6A5-coated beads captured doublecortin (*Dcx*), a well-known marker of neurogenesis in the human hippocampus (85); doublecortin-positive neurons are depleted in the hippocampal dentate gyrus in patients with Alzheimer disease (86). In view of the presence of B cell as well as T cell inflammatory responses in perinatal white matter injury (87), anti-PLP autoantibody-mediated mechanisms might also contribute to subsequent cerebral dysmaturation in those conditions (88).

CNS conditions in which myelin injury or degeneration is not overt may also show dysregulated adult neurogenesis (89). For example, perturbations of the identified anti-PLP mAb cell surface neuronal proteins, including altered expression of M6 proteins, are associated with depression (90–92), schizophrenia (92, 93), claustrophobia (94), chronic stress

(95), autism spectrum disorder (96, 97), and other psychiatric and neurodevelopmental conditions (92, 98, 99). Some of the molecules captured by the anti-PLP mAbs, (i.e. Ephs, NCAM and contactins), are also involved in post-seizure synaptogenesis in chronic epilepsy (100). In addition, Abs to neural antigens have been implicated in effects on CNS function in diseases not primarily of the CNS, for example cognitive impairment in rheumatoid arthritis (101, 102). Thus, the potential involvement of multispecific anti-PLP epitope Ab responses in these diverse disorders is considerable but remains to be investigated. Importantly, the effects of such Abs in chronic disease processes may differ from those in acute conditions (103).

Potential Implications for Therapeutic Neural Stem Cells

Neural and other stem cell regenerative therapies are currently intensively investigated for the treatment of MS, stroke, and many other neurological diseases (104–106). In this study, the anti-PLP mAb epitopes generally did not appear to be expressed in morphologically undifferentiated-appearing cell types either in the germinal matrix in the immature human brain specimens or in small round undifferentiated-appearing cells in the PC12 cell cultures in the absence of NGF (Supplementary Data Fig. S6). Moreover, no cytotoxic effects of the mAbs or apoptosis were observed in vitro. Therefore, although molecular mechanisms are not known, Ab effects in vivo would not likely be directly toxic but could affect stages of neuronal maturation, (including process elaboration, synapse formation, axon pathfinding, dendritic arborization, connectivity, etc.), which must be achieved by transplanted cells to restore normal neuronal functions. The presence of anti-PLP Abs that can inhibit these developmental processes might influence exogenous stem cell maturation thereby limiting their therapeutic efficacy in recipient patients.

Caveats in the Identification and Characterization of Anti-PLP Epitope Abs in Patients

In some studies, normal healthy and other neurological disease control patient samples have shown the same Ab reactivities, albeit at lower levels, as are found in some MS patient serum or CSF samples (56, 67, 68, 107). For example, anti-PLP peptide epitope Abs to both first and second loop regions were found in healthy controls (55), and in a patient with headache (48), respectively. Although these results suggest that such responses may neither be disease-specific nor critical to pathogenesis, several factors contribute to the failure to identify or accurately measure levels of anti-PLP epitope Abs in human CSF and other samples. The hydrophobicity of the PLP molecule overall, (and of individual peptides), and the lack of specific knowledge on the 3-dimensional conformation of the epitopes within myelin in vivo have been highlighted by Greer as confounding factors in characterizing T cell responses to PLP in MS patients that also apply to the assessment of anti-PLP epitope Abs (108). The spatial relationships of PLP and other pgf proteins with other myelin membrane

components are also not understood and the tetraspan structure of PLP makes characterization of immune responses to it versus those to other myelin molecules more challenging. The anti-PLP epitope Ab multispecificity demonstrated in this study may introduce further complexity to the quest for identification of individual disease-specific and other pathogenetic autoantigen Ab responses.

Multispecific anti-PLP epitope Abs might have also greater affinity for the native sequence or epitope conformation in myelin than to a neuronal precursor molecule to which they can cross-react. Even if there are no significant differences in Ab affinity, however, because PLP is the most abundant myelin protein, (e.g. approximately 17 times more abundant than MOG [2]), anti-PLP Abs, particularly those to external surface epitopes, would likely be bound by the overwhelmingly greater amounts of PLP in intact myelin throughout injured as well as normal CNS tissues. Such a "sponge effect" might preclude the identification or lower measured levels of anti-PLP epitope Abs in clinical specimens. Antibodies to less abundant myelin proteins and to those on the cytoplasmic myelin face, for example MBP, would be less likely to be bound by normal intact myelin. We are not aware evidence that anti-MBP, anti-MOG, or any other demyelinating disease-associated anti-myelin component mAb exhibits the same patterns of developmental immunostaining of neurons or neuronal precursor cells or the in vitro effects that we observed for the anti-PLP external face mAbs.

Some of the molecules present in myelin and captured by the anti-PLP mAbs in the IP experiments, for example integrins, Thy1, ECM molecules, and NCAM-1 (109), are also abundant in non-CNS tissues and could be bound by anti-PLP Abs in vivo both within and outside of the CNS thereby reducing their detectability. In the present study, neurite outgrowth inhibition was demonstrated using in vitro models with high dose, relatively short-term exposure of the mAbs to cells whereas lower concentrations over long time periods would likely be more relevant to mechanisms in chronic human diseases. In this regard, it is possible that transient exposure even to low levels of certain anti-PLP Abs can have long-term effects on the hippocampus; this has been suggested in a murine lupus autoantibody model (110). Thus, the failure to detect anti-PLP epitope Abs at a single time point in a serum or CSF sample may not preclude their pathobiological roles in chronic conditions. An additional caveat is that although PLP sequences among mammals are identical and the mAbs showed similar neuronal staining patterns in human and murine tissues (Supplementary Data tables in [3]), it is not known whether there are identical Ab epitope conformations of the identified captured PC12 cell molecules (other than of PLP) in humans or whether they have identical membrane topology and functions in the human CNS.

SUMMARY AND CONCLUSIONS

The results of this study indicate that: (i) in addition to their recognition of CNS myelin, anti-PLP mAbs to external face but not cytoplasmic face epitopes specifically recognize neurons in immature human CNS tissues, in adult human NSCN and in cultured developing mammalian cells with a

neuronal phenotype; (ii) mAbs to the external loop PLP epitopes capture neurodevelopmental membrane and ECM molecules both with, (i.e. M6 proteins), and without sequence similarities with PLP in IP experiments; and (iii) the anti-PLP mAb binding to the identified neuronal surface antigens correlates with but may not entirely account for their inhibition of neurodifferentiation in 2 in vitro models. These data represent an initial proof-of-principle that anti-myelin PLP epitope Ab recognition of neurodevelopmental antigens may affect the differentiation of neuronal precursor cells. They imply that similar inhibitory effects in vivo might contribute to impaired neuronal precursor cell differentiation in MS as well as other chronic neurological and psychiatric conditions. Validation of this hypothesis and a better understanding of the molecular mechanisms of multispecific anti-PLP Ab effects may lead to the development of appropriate diagnostic and therapeutic strategies.

REFERENCES

1. Greer JM, Lees MB. Myelin proteolipid protein—The first 50 years. Int J Biochem Cell Biol 2002;34:211–5
2. Jahn O, Tenzer S, Werner HB. Myelin proteomics: Molecular anatomy of an insulating sheath. Mol Neurobiol 2009;40:55–72
3. Greenfield EA, Reddy J, Lees A, et al. Monoclonal antibodies to distinct regions of human myelin proteolipid protein simultaneously recognize central nervous system myelin and neurons of many vertebrate species. J Neurosci Res 2006;83:415–31
4. Kempermann G, Song H, Gage FH. Neurogenesis in the adult hippocampus. Cold Spring Harb Perspect Biol 2015;7:a018812
5. Tanos T, Saibene AM, Pipolo C, et al. Isolation of putative stem cells present in human adult olfactory mucosa. PLoS One 2017;12:e0181151
6. Kitagawa K, Sinoway MP, Yang CP, et al. A proteolipid protein gene family: Expression in sharks and rays and possible evolution from an ancestral gene encoding a pore-forming polypeptide. Neuron 1993;11:433–8
7. Stecca B, Southwood CM, Gragerov A, et al. The evolution of lipophilin genes from invertebrates to tetrapods: DM-20 cannot replace proteolipid protein in CNS myelin. J Neurosci 2000;20:4002–10
8. James LC, Tawfik DS. Conformational diversity and protein evolution—A 60-year-old hypothesis revisited. Trends Biochem Sci 2003;28:361–8
9. Lagenaur C, Kunemund V, Fischer G, et al. Monoclonal M6 antibody interferes with neurite extension of cultured neurons. J Neurobiol 1992;23:71–88
10. Roussel G, Trifilieff E, Lagenaur C, et al. Immunoelectron microscopic localization of the M6a antigen in rat brain. J Neurocytol 1998;27:695–703
11. Werner H, Dimou L, Klugmann M, et al. Multiple splice isoforms of proteolipid M6B in neurons and oligodendrocytes. Mol Cell Neurosci 2001;18:593–605
12. Mukobata S, Hibino T, Sugiyama A, et al. M6a acts as a nerve growth factor-gated $Ca2^+$ channel in neuronal differentiation. Biochem Biophys Res Commun 2002;297:722–8
13. Mita S, de Monasterio-Schrader P, Fünfschilling U, et al. Transcallosal projections require glycoprotein M6-dependent neurite growth and guidance. Cereb Cortex 2015;25:4111–25
14. Ito Y, Honda A, Igarashi M. Glycoprotein M6a as a signaling transducer in neuronal lipid rafts. Neurosci Res 2018;128:19–24
15. Rosas NM, Alvarez JA, Alzuri SE, et al. Alanine scanning mutagenesis of the C-terminal cytosolic end of Gpm6a identifies key residues essential for the formation of filopodia. Front Mol Neurosci 2018;11:314
16. Yamamura T, Konola JT, Wekerle H, et al. Monoclonal antibodies against myelin proteolipid protein: Identification and characterization of two major determinants. J Neurochem 1991;57:1671–80
17. The UniProt Consortium. UniProt: The universal protein knowledgebase. Nucleic Acids Res 2017;45:D158–69
18. Weidenheim KM, Bodhireddy SR, Rashbaum WK, et al. Temporal and spatial expression of major myelin proteins in the human fetal spinal cord during the second trimester. J Neuropathol Exp Neurol 1996;55:734–45
19. Vaudry D, Stork PJD, Lazarovici P, et al. Signaling pathways for PC12 cell differentiation: Making the right connections. Science 2002;296:1648–9
20. Ikenaka K, Kagawa T, Mikoshiba K. Selective expression of DM-20, an alternatively spliced myelin proteolipid protein gene product, in developing nervous system and in nonglial cells. J Neurochem 1992;58:2248–53
21. Michalski JP, Anderson C, Beauvais A, et al. The proteolipid protein promoter drives expression outside of the oligodendrocyte lineage during embryonic and early postnatal development. PLoS One 2011;6:e19772
22. Harlow DE, Saul KE, Culp CM, et al. Expression of proteolipid protein gene in spinal cord stem cells and early oligodendrocyte progenitor cells is dispensable for normal cell migration and myelination. J Neurosci 2014;34:1333–43
23. Harlow DE, Saul KE, Komuro H, et al. Myelin proteolipid protein complexes with αv integrin and AMPA receptors in vivo and regulates AMPA-dependent oligodendrocyte progenitor cell migration through the modulation of cell-surface GluR2 expression. J Neurosci 2015;35:12018–32
24. Lüders KA, Patzig J, Simons M, et al. Genetic dissection of oligodendroglial and neuronal Plp1 function in a novel mouse model of spastic paraplegia type 2. Glia 2017;65:1762–76
25. Inoue K. PLP1-related inherited dysmyelinating disorders: Pelizaeus-Merzbacher disease and spastic paraplegia type 2. Neurogenetics 2005;6:1–16
26. Qendro V, Bugos GA, Lundgren DH, et al. Integrative proteomics, genomics, and translational immunology approaches reveal mutated forms of Proteolipid Protein 1 (PLP1) and mutant-specific immune response in multiple sclerosis. Proteomics 2017;17:doi: 10.1002/pmic.201600322
27. Cloake NC, Yan J, Aminian A, et al. PLP1 mutations in patients with multiple sclerosis: Identification of a new mutation and potential pathogenicity of the mutations. JCM 2018;7:pii:E342
28. Miller MJ, Haxhiu MA, Georgiadis P, et al. Proteolipid protein gene mutation induces altered ventilatory response to hypoxia in the myelin-deficient rat. J Neurosci 2003;23:2265–73
29. Shimokawa N, Dikic I, Sugama S, et al. Molecular responses to acidosis of central chemosensitive neurons in brain. Cell Signal 2005;17:799–808
30. Miller MJ, Kangas CD, Macklin WB. Neuronal expression of the proteolipid protein gene in the medulla of the mouse. J Neurosci Res 2009;87:2842–53
31. Jacobs EC, Bongarzone ER, Campagnoni CW, et al. Soma-restricted products of the myelin proteolipid gene are expressed primarily in neurons in the developing mouse nervous system. Dev Neurosci 2003;25:96–104
32. Christian KM, Song H, Ming G-l. Functions and dysfunctions of adult hippocampal neurogenesis. Annu Rev Neurosci 2014;37:243–62
33. Bergmann O, Spalding KL, Frisén J. Adult neurogenesis in humans. Cold Spring Harb Perspect Biol 2015;7:a018994
34. Ihunwo AO, Tembo LH, Dzamalala C. The dynamics of adult neurogenesis in human hippocampus. Neural Regen Res 2016;11:1869–83
35. Boldrini M, Fulmore CA, Tartt AN, et al. Human hippocampal neurogenesis persists throughout aging. Cell Stem Cell 2018;22:589–99
36. Baptista P, Andrade JP. Adult hippocampal neurogenesis: Regulation and possible functional and clinical correlates. Front Neuroanat 2018;12:44

37. Fuchsova B, Fernández ME, Alfonso J, et al. Cysteine residues in the large extracellular loop (EC2) are essential for the function of the stress-regulated glycoprotein M6a. J Biol Chem 2009;284:32075–88

38. Zhou Z-H, Tzioufas AG, Notkins AL. Properties and function of poly-reactive antibodies and polyreactive antigen-binding B cells. J Autoimmun 2007;29:219–28

39. Marchalonis JJ, Adelman MK, Robey IF, et al. Exquisite specificity and peptide epitope recognition promiscuity, properties shared by antibodies from sharks to humans. J Mol Recognit 2001;14:110–21 (Review)

40. Van Regenmortel M. Specificity, polyspecificity, and heterospecificity of antibody-antigen recognition. J Mol Recognit 2014;27:627–39

41. James LC, Roversi P, Tawfik DS. Antibody multispecificity mediated by conformational diversity. Science 2003;299:1362–7

42. Avrameas S, Alexopoulos H, Moutsopoulos HM. Natural autoantibodies: An undersung hero of the immune system and autoimmune disorders—A point of view. Front Immunol 2018;9:1320

43. James LC, Tawfik DS. The specificity of cross-reactivity: Promiscuous antibody binding involves specific hydrogen bonds rather than nonspecific hydrophobic stickiness. Protein Sci 2009;12:2183–93

44. Mitsdoerffer M, Peters A. Tertiary lymphoid organs in central nervous system autoimmunity. Front Immunol 2016;7:451

45. Warren KG, Catz I, Johnson E, et al. Anti-myelin basic protein and anti-proteolipid protein specific forms of multiple sclerosis. Ann Neurol 1994;35:280–9

46. Sellebjerg F, Jensen CV, Christiansen P. Intrathecal IgG synthesis and autoantibody-secreting cells in multiple sclerosis. J Neuroimmunol 2000;108:207–15

47. Carvalho A, Sant'anna G, Santos CC, et al. [Determination of autoantibody for myelin antigens in the serum of patients HLA-DQB1*0602 with multiple sclerosis]. Arq Neuropsiquiatr 2003;61:968–73

48. Ousman SS, Tomooka BH, Van Noort M, et al. Protective and therapeutic role for α-B-crystallin in autoimmune demyelination. Nature 2007;448:474–9

49. Greer JM, Csurhes PA, Muller DM, et al. Reactivity to myelin proteins with HLA type correlation of blood T cell and antibody and lesion localization in multiple sclerosis. J Immunol 2008;180:6402–10

50. Jaśkiewicz E, Michałowska-Wender G, Pyszczek A, et al. Recombinant forms of myelin antigens expressed on Chinese hamster ovary (CHO) cells as a tool for identification of autoantibodies in serum of multiple sclerosis patients. Folia Neuropathol 2010;48:45–8

51. Quintana FJ, Farez MF, Izquierdo G, et al. Antigen microarrays identify CNS-produced autoantibodies in RRMS. Neurology 2012;78:532–9

52. Van Haren K, Tomooka BH, Kidd BA, et al. Serum autoantibodies to myelin peptides distinguish acute disseminated encephalomyelitis from relapsing-remitting multiple sclerosis. Mult Scler J 2013;19:1726–33

53. Fraussen J, Claes N, de Bock L, et al. Targets of the humoral autoimmune response in multiple sclerosis. Autoimmun Rev 2014;13:1126–37

54. Metz I, Beißbarth T, Ellenberger D, et al. Serum peptide reactivities may distinguish neuromyelitis optica subgroups and multiple sclerosis. Neurol Neuroimmunol Neuroinflamm 2016;3:e204

55. Zamanzadeh Z, Ahangari G, Ataei M, et al. Association of new putative epitopes of myelin proteolipid protein (58-74) with pathogenesis of multiple sclerosis. Iran J Allergy Asthma Immunol 2016;15:394–402

56. Willis SN, Stathopoulos P, Chastre A, et al. Investigating the antigen specificity of multiple sclerosis central nervous system-derived immunoglobulins. Front Immunol 2015;6:600

57. Brändle SM, Obermeier B, Senel M, et al. Distinct oligoclonal band antibodies in multiple sclerosis recognize ubiquitous self-proteins. Proc Natl Acad Sci USA 2016;113:7864–9

58. Winger RC, Zamvil SS. Commentary. Antibodies in multiple sclerosis oligoclonal bands target debris. Proc Natl Acad Sci USA 2016;113:7696–8

59. Eshaghi A, Prados F, Brownlee WJ, et al. Deep gray matter volume loss drives disability worsening in multiple sclerosis. Ann Neurol 2018;83:210–22

60. Charles P, Reynolds R, Seilhean D, et al. Re-expression of PSA-NCAM by demyelinated axons: An inhibitor of remyelination in multiple sclerosis? Brain 2002;125:1972–9

61. Syed YA, Zhao C, Mahad D, et al. Antibody-mediated neutralization of myelin-associated EphrinB3 accelerates CNS remyelination. Acta Neuropathol 2016;131:281–98

62. Barros CS, Franco SJ, Müller U. Extracellular matrix: Functions in the nervous system. Cold Spring Harb Perspect Biol 2011;3:a005108

63. Zhang Y, Da R-R, Guo W, et al. Axon reactive B cells clonally expanded in the cerebrospinal fluid of patients with multiple sclerosis. J Clin Immunol 2005;25:254–64

64. Sobel RA. Ephrin A receptors and ligands in lesions and normal-appearing white matter in multiple sclerosis. Brain Pathol 2006;15:35–45

65. Gnanapavan S, Ho P, Heywood W, et al. Progression in multiple sclerosis is associated with low endogenous NCAM. J Neurochem 2013;125:766–73

66. Blauth K, Soltys J, Matschulat A, et al. Antibodies produced by clonally expanded plasma cells in multiple sclerosis cerebrospinal fluid cause demyelination of spinal cord explants. Acta Neuropathol 2015;130:765–81

67. Prineas JW, Parratt J. Multiple sclerosis: Serum anti-CNS autoantibodies. Mult Scler J 2018;24:610–22

68. Hecker M, Fitzner B, Wendt M, et al. High-density peptide microarray analysis of IgG autoantibody reactivities in serum and cerebrospinal fluid of multiple sclerosis patients. Mol Cell Proteomics 2016;15:1360–80

69. Gennarini G, Bizzoca A, Picocci S, et al. The role of Gpi-anchored axonal glycoproteins in neural development and neurological disorders. Mol Cell Neurosci 2017;81:49–63

70. Rivas JR, Ireland SJ, Chkheidze R, et al. Peripheral VH4+ plasmablasts demonstrate autoreactive B cell expansion toward brain antigens in early multiple sclerosis patients. Acta Neuropathol 2017;133:43–60

71. Papadopoulos D, Dukes S, Patel R, et al. Substantial archaeocortical atrophy and neuronal loss in multiple sclerosis. Brain Pathol 2009;19:238–53

72. Dutta R, Chang A, Doud MK, et al. Demyelination causes synaptic alterations in hippocampi from multiple sclerosis patients. Ann Neurol 2011;69:445–54

73. Koenig KA, Sakaie KE, Lowe MJ, et al. Hippocampal volume is related to cognitive decline and fornicial diffusion measures in multiple sclerosis. Magn Reson Imaging 2014;32:354–8

74. Yaldizli Ö, Penner IK, Yonekawa T, et al. The association between olfactory bulb volume, cognitive dysfunction, physical disability and depression in multiple sclerosis. Eur J Neurol 2016;23:510–9

75. Oreja-Guevara C, Gómez-Pinedo U, García-López J, et al. Inhibition of neurogenesis in a case of Marburg variant multiple sclerosis. Mult Scler Relat Disord 2017;18:71–6

76. Kesidou E, Touloumi O, Lagoudaki R, et al. Humoral response in experimental autoimmune encephalomyelitis targets neural precursor cells in the central nervous system of naïve rodents. J Neuroinflamm 2017;14:227

77. Dalmau J, Geis C, Graus F. Autoantibodies to synaptic receptors and neuronal cell surface proteins in autoimmune diseases of the central nervous system. Physiol Rev 2017;97:839–87

78. Ankeny DP, Popovich PG. B cells and autoantibodies: Complex roles in CNS injury. Trends Immunol 2010;31:332–8

79. Kobeissy F, Moshourab RA, Autoantibodies in CNS trauma and neuropsychiatric disorders. A new generation of biomarkers. In: Kobeissy FH, ed. Brain Neurotrauma: Molecular, Neuropsychological, and Rehabilitation Aspects. Boca Raton, FL: CRC Press/Taylor & Francis 2015.

80. Schneider L, Reichert E, Faulkner J, et al. CNS inflammation and neurodegeneration: Sequelae of peripheral inoculation with spinal cord tissue in rat. J Neurosurg 2019;1–12. doi: 10.3171/2018.10.JNS181517

81. Doyle KP, Quach LN, Solé M, et al. B-lymphocyte-mediated delayed cognitive impairment following stroke. J Neurosci 2015;35:2133–45

82. Becker KJ, Tanzi P, Zierath D, et al. Antibodies to myelin basic protein are associated with cognitive decline after stroke. J Neuroimmunol 2016;295–6:9–11

83. Kandasamy M, Aigner L. Neuroplasticity, limbic neuroblastosis and neuro-regenerative disorders. Neural Regen Res 2018;13:1322–6

84. Papuć E, Kurys-Denis E, Krupski W, et al. Can antibodies against glial derived antigens be early biomarkers of hippocampal demyelination and memory loss in Alzheimer's disease? JAD 2015;48:115–21

85. Kuhn HG, Toda T, Gage FH. Progressions. Adult hippocampal neurogenesis: A coming-of-age story. J Neurosci 2018;38:10401–10

86. Moreno-Jiménez EP, Flor-García M, Terreros-Roncal J, et al. Adult hippocampal neurogenesis is abundant in neurologically healthy

subjects and drops sharply in patients with Alzheimer's disease. Nat Med 2019;25:554–60

87. Nazmi A, Albertsson AM, Rocha-Ferreira E, et al. Lymphocytes contribute to the pathophysiology of neonatal brain injury. Front Neurol 2018;9:159

88. Back SA, Miller SP. Brain injury in premature neonates: A primary cerebral dysmaturation disorder? Ann Neurol 2014;75:469–86

89. Yun S, Reynolds RP, Masiulis I, et al. Re-evaluating the link between neuropsychiatric disorders and dysregulated adult neurogenesis. Nat Med 2016;11:1239–47

90. Fuchsova B, Alvarez JA, Rizavi HS, et al. Altered expression of neuroplasticity-related genes in the brain of depressed suicides. Neuroscience 2015;299:1–17

91. Zong S, Hoffmann C, Mané M, et al. Neuronal surface autoantibodies in neuropsychiatric disorders: Are there implications for depression? Front Immunol 2017;8:752

92. Hawi Z, Tong J, Dark C, et al. The role of cadherin genes in five major psychiatric disorders: A literature update. Am J Med Genet 2018;177B:168–80

93. Barbeau D, Liang JJ, Robitalille Y, et al. Decreased expression of the embryonic form of the neural cell adhesion molecule in schizophrenic brains. Proc Natl Acad Sci USA 1995;92:2785–9

94. El-Kordi A, Kästner A, Grube S, et al. A single gene defect causing claustrophobia. Transl Psychiatry 2013;3:e254

95. Alfonso J, Fernández ME, Cooper B, et al. The stress-regulated protein M6a is a key modulator for neurite outgrowth and filopodium/spine formation. Proc Natl Acad Sci USA 2005;102:17196–201

96. Guang S, Pan N, Deng X, et al. Synaptopathology involved in autism spectrum disorder. Front Cell Neurosci 2018;12:470

97. Chatterjee M, Schild D, Teunissen CE. Contactins in the central nervous system: Role in health and disease. Neural Regen Res 2019;14:206–16

98. Hirabayashi T, Yagi T. Protocadherins in neurological diseases. Adv Neurobiol 2014;8:293–314

99. Guemez-Gamboa A, Çağlayan AO, Stanley V, et al. Loss of protocadherin-12 leads to diencephalic-mesencephalic junction dysplasia syndrome. Ann Neurol 2018;84:646–55

100. Gorlewicz A, Kaczmarek L. Pathophysiology of trans-synaptic adhesion molecules: Implications for epilepsy. Front Cell Dev Biol 2018;6:119

101. Baptista TSA, Petersen LE, Molina JK, et al. Autoantibodies against myelin sheath and S100β are associated with cognitive dysfunction in patients with rheumatoid arthritis. Clin Rheumatol 2017;36:1959–68

102. Bashford-Rogers RJM, Smith KGC, Thomas DC. Antibody repertoire analysis in polygenic autoimmune diseases. Immunology 2018;155:3–17

103. Ludwig RJ, Vanhoorelbeke K, Leypoldt F, et al. Mechanisms of autoantibody-induced pathology. Front Immunol 2017;8:603

104. Rolfe A, Sun D, Stem cells for trauma: Stem cell therapy in brain trauma: Implications for repair and regeneration of injured brain in experimental TBI models. In: Kobeissy FH, ed. Brain Neurotrauma: Molecular, Neuropsychological, and Rehabilitation Aspects. Boca Raton, FL: CRC Press/Taylor & Francis 2015.

105. Scolding NJ, Pasquini M, Reingold, SC, et al. Cell-based therapeutic strategies for multiple sclerosis. Brain 2017;140:2776–96

106. Levy M, Boulis N, Rao M, et al. Regenerative cellular therapies for neurologic diseases. Brain Res 2016;1638:88–96

107. Amor S, Peferoen LAN, Vogel DYS, et al. Inflammation in neurodegenerative diseases—An update. Immunology 2014;142:151–66

108. Greer JM. Autoimmune T-cell reactivity to myelin proteolipids and glycolipids in multiple sclerosis. Mult Scler Int 2013;2013:151427

109. Quartu M, Serra MP, Boi M, et al. Polysialylated-neural cell adhesion molecule (PSA-NCAM) in the human trigeminal ganglion and brainstem at prenatal and adult ages. BMC Neurosci 2008;9:108

110. Nestor J, Arinuma Y, Huerta TS, et al. Lupus antibodies induce behavioral changes mediated by microglia and blocked by ACE inhibitors. J Exp Med 2018;215:2554–66